Recent advances in embedded technologies and self-sensing concrete for structural health monitoring

Received: 30 May 2024 | Revised: 11 August 2024 | Accepted: 14 August 2024

DOI: 10.1002/suco.202400714

ARTICLE

fib CEB-FIP WILEY

Recent advances in embedded technologies and self-sensing concrete for structural health monitoring

Marco Civera | **Ahmad Naseem** | **Bernardino Chiaia**

Department of Structural, Building and Geotechnical Engineering, Politecnico di Torino, Turin, Italy

Correspondence
Marco Civera, Department of Structural, Building and Geotechnical Engineering, Politecnico di Torino, Corso Duca degli Abruzzi 24, 10129 Turin, Italy.
Email: marco.civera@polito.it

Funding information
NextGenerationEU

Abstract

Fully embedded and spatially diffuse sensors are central to the advancement of civil and construction engineering. Indeed, they serve as an enabling technology necessary for addressing the current challenges associated with through-life management and structural health monitoring of existing structures and infrastructures. The need to identify structural issues early on has driven the integration of such embedded sensing capabilities into construction materials, turning passive structures into proactive, self-aware "entities," commonly referred to as Smart Structures. The economic rationale behind this endeavor is underscored by the vital significance of continuous monitoring, which enables prompt anomaly assessment and thus mitigates the risks of potential structural failures. This is particularly relevant for road and rail infrastructures, as they represent a substantial and enduring investment for any nation. Given that a large majority of these large infrastructures are composed of concrete and reinforced concrete, both academics and construction companies are continuously researching micro- and nano-engineered self-sensing solutions specifically tailored for this building material. This comprehensive review paper reports the latest advances in the field of self-sensing concrete as of 2024, with an emphasis on intrinsic self-sensing concrete, that is, electrically conductive functional fillers. A critical analysis and a discussion of the findings are provided. Based on the perceived existing gaps and demands from the industry, the field's future perspectives are also briefly outlined.

KEYWORDS

carbon nanotubes, embedded sensors, self-sensing concrete, smart concrete, structural health monitoring

1 | INTRODUCTION

The most widely accepted interpretation of the term "Smart Structure" in the current scientific literature is *"the ability of structural members to sense, diagnose, and actuate in order to perform their functions."*[1] While the embedment of conventional actuators is still mostly limited to aerospace and mechanical engineering applications to metallic or alloy structures,[2] this research field has rapidly expanded to civil engineering in the last decade, in terms of self-sensing building materials. Hence, fully embedded and diffused sensors are a key enabling technology for this next generation of buildings, bridges, tunnels, and other kinds of civil structures and infrastructures.

Due to the perceived potential of this framework, applications to self-sensing asphalt pavements[3–5] and clay bricks[6,7] have been proposed for a variety of tasks, from embedded weigh-in-motion[8] to strain monitoring.[9,10] Thanks to integrated sensing capabilities, these and other common construction materials can be enhanced to become part of the so-called "Smart Materials."[11] In this review study, the focus will be on conventional concrete and reinforced concrete (RC) as well as derived materials such as steel-fiber-RCs[12] and ultra-high-performance concrete (UHPC), also known as ultra-high strength concrete (UHSC).[13] Eventually, all these embedded sensing capabilities are intended to address issues such as the assessment of concrete durability[14] and corrosion monitoring.[15,16]

This gradual transition from traditional construction and monitoring methods to new integrated solutions is made possible by new advancements in sensor technology and materials. The motivations behind this trend stem from the ever-rising interest in structural health monitoring (SHM[17]), that is, the use of sensed physical properties—mainly linked to the vibrational response of the target system—to assess the damage occurrence and growth inside the material via vibration-based diagnosis.[18,19] In this regard, civil infrastructure is one of the most expensive investments a country can make. These structures have a long service life and thus require prolonged and constant maintenance, which in turn necessitates a significant amount of time and resources. Nowadays, destructive or nondestructive test (NDT) procedures are most commonly employed to evaluate a structure's condition. Yet, NDT approaches include taking complex and expensive instrumentation and tools to periodically perform on-site inspections. The fact that present techniques' tests only provide local information about a small portion of the entire structure, most often limited to the outermost layers, rather than its global and/or interior integrity, is another issue. Conversely, the goal of SHM is to provide an automated system for permanent and continuous damage detection, assessment, and diagnosis, by reducing the need for manned maintenance—and thus, labor costs—while increasing the chance of detecting significant damage in load-bearing elements.[20] In this framework, SHM and Smart Structures can be considered in the optics of Internet of Things (IoT) technology integration as well.[21]

In these terms, it is not uncommon to refer to current SHM hardware apparatuses as "embedded systems"; nevertheless, the term is often used (potentially improperly) as a synonym for "permanently installed" networks of surface-mounted, physically attached sensors. Instead, by providing a permanent, unmovable, and continuous sensing solution, actual construction material-embedded sensors are the natural evolution of the SHM concept. From all these considerations arises the significance of integrating sensors (of various kinds) inside concrete and RC. Another major advantage would be the possibility to potentially monitor any geometric point of the RC structure, wherever concrete is cast, indepentently of its accessibility after construction.

1.1 | Paper organization, objectives, and research method

1.1.1 | Objectives and paper organization

Having outlined the relevance of the topic, the objective of this study is threefold: to review the current state-of-the-art, to identify and address existing issues, and finally to compare and evaluate the applicability of current self-sensing concrete (SSC) technologies. The organization of the paper follows this logical flow: after some essential recalls on the fundamental aspects of Smart Structures (Section 2), recent advances in sensors, dispersion methods, and data acquisition technologies are presented and commented upon in Section 3 (regarding laboratory-tested applications) and Section 4 (regarding field applications). Based on this critical review of the literature, key considerations regarding the main parameters for functional and efficient Smart Concrete solutions are highlighted in Section 5. Conversely, challenges, research gaps, and technical limitations of SSC "as-is" and its application in the industry are studied in Section 6. This helps to contribute toward academic and industrial research areas that require further exploration. The Conclusions (Section 7) end this work.

1.1.2 | Research methodology

The following search engines were used: Google Scholar, Scopus, and Web of Science. The keywords included: "Self-sensing concrete," "Nano-engineered concrete," "Embedded Sensors," "Carbon Nanotubes (CNTs)," "Smart concrete," and "Carbon-nanotubes based composite." To widen the research, more general keywords such as "Nanotechnology," "Civil Engineering", "Fiber-optic Sensors", "Piezoresistive Sensors", "Electrical Impedance Tomography", "EIT", and others were added to the previous list. The temporal limitation was set between 1995 and 2024, thus covering both the recent developments as well as historic ones in the last 30 years. However, more emphasis were put on the last 5 years, as pre-2020 works were partially covered by Reference 22, which aimed more specifically at carbon nanofibers (CNFs) and nanotubes and thus more circumscribed in its discussion. This resulted in more than 360 peer-reviewed works; these were then selected based on their title and abstract, reaching a final selection of slightly more than 130 papers

deemed of major interest and discussed in this text. The majority of this work covers the topic of intrinsically self-sensing concretes (ISSC), while a minority of them discusses non-intrinsically alternatives (these two terms will be better introduced in Section 2.1). Other works on related topics have been added as well to provide the needed context, reaching the definitive form of the provided reference list. As a potential publication bias, it must be stated that this research was limited to published and peer-reviewed documents. Preprints were not considered. Thus, there might be some latest, ongoing, or unpublished research which might not be included.

1.1.3 | Eligibility criteria

This review focused primarily, but not exclusively, on experimental studies. Numerical simulation studies predicting the conductivity or resistivity of SSC were evaluated on a case-by-case basis but mostly excluded to maintain an emphasis on empirical evidence. Numerical models based on parameters like fiber length and thickness to simulate self-sensing behavior were not considered. Similarly, purely theoretical studies based on hypotheses are largely omitted. Again, this is intended to preserve the focus on the applicability of SSC.

2 | FUNDAMENTALS OF SMART STRUCTURES

To provide the readers with the needed background, a few important concepts are recalled in this section.

2.1 | Intrinsic and non-intrinsic self-sensing concrete

First of all, it is important to highlight that SSC encompasses two main groups: ISSC and non-intrinsic self-sensing concrete (NISSC). Basically, the difference lies in that NISSC refers to concrete that uses external sensors or actuators integrated into it to enable sensing functions,[23] rather than relying on the inherent conductive properties of materials poured into the concrete mix itself.[21] In ISSC—also known as self-monitoring, intrinsically smart, piezoresistive, or pressure-sensitive concrete—functional fillers are incorporated into the concrete matrix. A concise and accurate definition of ISSC is given in Reference 23: "*A structural material that can monitor itself without the need of embedded, attached, or remote sensors*". This research field flourished since Chen', Chuang', and coauthors' groundbreaking research works in the early 1990s, which revealed the self-sensing cementitious composites with short-cut carbon fibers (CFs).[24–27]

Other filler materials include steel fibers (SFs),[28] carbon nanotubes (CNTs),[29] nickel powder (NP), nanoscale graphite powder (GP), carbon black (CB/CNB), and others.[30] The addition of these functional fillers enables the concrete's ability to sense and monitor various parameters, such as strain and crack occurrence/crack growth while trying to maintain—or potentially even improve—its mechanical properties and durability. In this regard, the core concepts of ISSC are:

i. the ability of the functional filler to change the overall conductivity of the final product, and
ii. the ability of this resulting concrete to generate perceivable electric charges under mechanical loads.[31]

Recalling some basic concepts of electrical engineering, the electrical resistivity ρ, measured in ohm-meters (Ωm), is defined as the measure of a target object's ability to resist the flow of electric current, that is

$$\rho = \frac{RA}{l}, \tag{1}$$

where R is the material resistance in ohm (Ω), A the cross-sectional area transversal to the current flow in square meters (m^2), and l is the length in meters (m). The material conductivity is the inverse of Equation (1), being

$$\sigma = \frac{1}{\rho}, \tag{2}$$

expressed in siemens per meter (S/m). Concrete's electrical resistance varies widely depending on various factors such as its water–cement ratio, porosity, pore structure, cement composition, presence of rebar steel, moisture content, and external ambient temperature. However, generally speaking, it is always quite high w.r.t. to good conductors such as metals. It ranges from a minimum of $\rho \cong 1\,\Omega$m for freshly poured concrete[32] to $10^2 - 10^3\,\Omega$m for wet fully cured concrete and $10^6 - 10^{10}\,\Omega$m when dry at high temperatures.[33] For outdoor dried concrete, it is most commonly attested between 6.54×10^3 and $11.4 \times 10^3\,\Omega$m.[34] However, these values are general estimates and can vary based on the specific conditions and materials used, especially if certain types of aggregates are purposefully added to lower the resistance.

Hence, the idea is to reduce the global resistance of the cement mix via a conductive network of highly conductive filler material, dispersed in the mix. As the concrete structure deformates, the dispersed filler changes its

shape as well, slightly modifying its conductivity. These changes in the conductive network are at the base of resistance-based sensing which, despite some improvements in alternative methodologies such as capacitance-based sensing,[35] remains to date the most common approach.

In this framework, the fractional change in (longitudinal) electrical resistivity (FCR), defined as the ratio between the change in resistivity over its initial value, that is, $\Delta\rho/\rho_0$, acts as a proxy index for the mechanical parameters of interest. The rationale is that FCR is directly proportional to the fractional change in length $\Delta L/L_0$, that is, the axial strain ε, by a factor known as gauge factor (GF). Importantly, this makes ISSC solutions theoretically viable for an all-encompassing load range. As will be discussed more in detail in Section 5.1, changes in FCR can be appreciated both in the early elastic and subsequent plastic deformation regions. In the end, the final increase in electrical resistance continues even beyond the failure threshold of the ISSC.[36,37] These considerations apply to the three main load types to which R.C. structural elements are generally subject to—uniaxial compression, uniaxial tension, and pure bending.

Before continuing, the two concepts of percolation threshold and polarization effects need to be introduced as well, to understand the working principles of functional fillers in ISSC.

The percolation threshold is an optimum concentration of the incorporated material which forms conductive networks or pathways within the composite mix—that is to say, of the conductive functional filler. After this critical value is reached, a continuous conductive network is formed, enabling the material as a whole to become electrically conductive. Instead, the mix acts as an insulator when the filler concentration is below this threshold. In fact, cement has near-insulating or low electrical conductivity by nature.[38] Achieving a low percolation threshold is desirable, as it reduces the amount of expensive conductive fillers (like CFs, CNTs, graphene, etc.) required to impart self-sensing capabilities to the concrete. Each functional filler has its own native percolation threshold (e.g., generally lower for CFs and CNTs than CB). Yet, that can be modified, for instance, with the use of admixtures to influence the electrical properties of the concrete mix. The percolation threshold is generally indicated as either percentage by volume, vol.%, or percentage by mass/weight, wt.%.

The polarization of the cement paste has a significant impact on the electrical, and thus self-sensing properties, of the resulting concrete. Nevertheless, it can also affect its mechanical properties, not necessarily in a positive or harmless way—potentially it can also cause a decrease in the ultimate compressive strength.[39] Polarization effects in self-sensing materials are distinguishable in both alternating current (AC) and direct current (DC) circuits. In DC circuits, polarization is constant, while in AC circuits, it fluctuates with the AC. This is important for understanding the material response under different electrical conditions[40]; for this reason, experiments are often conducted in various electric fields (both DC and AC with various frequencies).

These aspects represent the most focal points, briefly summarized. Many relevant points and deeper discussions about the principles of ISSC can also be found in Reference 41.

Thus, the conductive fillers can be categorized according to their basic material (e.g., graphene derivative, carbon-based, etc.), their size (nano or micro materials), and geometry (powder, amorphous, or fibrous). Their mechanical and electrical properties and main characteristics can be summarized as follows:

- SFs are short, discrete fibers of steel with aspect ratio ranging from 20 to 100. Generally, they can be either twisted, straight, or hooked-ended. The incorporation of these fibers is possible within the composite matrix due to their small size which in turn alters the mechanical and electrical properties.[39] They are flexible and very cost-effective, but due to their macroscopic size, they can be challenging in concrete mixing. Also, they have a relatively low electrical conductivity, especially in comparison with other alternatives reported below.
- CFs are the most used functional fillers for SSC due to their unique combination of mechanical and electrical properties.[40] In particular, they have a very low percolation threshold, generally around 0.27–0.30 vol.%[41] They are much easier to mix and embed than SFs; however, as with all the other conductive fillers, uniform dispersion is important to achieve a consistent conductive network. In comparison to SFs, they have much less flexibility, higher conductivity, and higher preparation costs. They are also prone to corrosion.
- CNTs can be either single-walled (SWCNTs) or multi-walled (MWCNTs). Both have been used in experimentations to study their properties and their effect on the resistivity of the composite matrix. Notably, they show very good mechanical strength and electrical conductivity, due to a combination of a nanometric size for a high aspect ratio and surface area. Furthermore, they can be dispersed at low concentrations, as their percolation threshold is generally low, similar to CFs (ca. 2–4 wt.%).[41] Nevertheless, CNTs are prone to agglomeration and thus their uniform dispersion needs to be carried out through dispersion methods.[42] Good

alignment is difficult to achieve as well. Also, MWCNTs and CWCNTs work in such a way that they show variations in material properties under the influence of external forces. Strictly related to CNTs, CNFs are produced in a similar manner. However, they can or cannot be hollowed and are generally larger in size (up to a few μm in diameter), thus less oriented, more disordered, and sometimes losing their concentrical structure, while also having some defects, which are instead mostly absent from CNTs.

- NPs, due to their spiky spherical shape, have excellent conductivity due to the field emission effect on the nanotips.[44] Furthermore, differently from fibrous or nanoscale carbon material with suboptimal specific surface area and aspect ratio, recent research works[45] showed that NP does not need any special surfactant to remove aggregation and entanglement. Nevertheless, its percolation threshold is typically high, around 10–15 vol.% for the best self-sensing properties in concrete.[46] However, higher nickel contents above the percolation threshold can lead to decreased mechanical strength due to increased porosity.
- Nanoscale GPs are granular with very fine grain size (d_{50} about 15.5 μm[47]). However, they present some drawbacks and limitations. First, as for many powder-based conductive fillers, they need a dispersing agent to obtain a homogenous suspension; other additives are required to avoid the formation of large pores due to air entrapped during mixing. Second, they have a relatively high percolation threshold at ca. 10–12 wt.%, also depending on the compressive stress applied.[47] Furthermore, higher graphite contents above the percolation threshold can lead to decreased mechanical strength due to increased porosity. Other graphene derivatives, like reduced graphene oxide, are also used as conductive fillers.
- CB, a form of amorphous carbon, is another material that is widely used in ISSC due to its high surface-area-to-volume ratio and conductivity. It is a powdered-based substance with a size between 50 and 500 nm, obtained as a result of incomplete combustion of coal.[48] For this reason, it has a much lower preparation cost than CFs or CNTs. It is remarkably easier to disperse in concrete mixtures. However, CB is prone to agglomeration. As before, the dispersion of CB is of prime importance in order to effectively maintain a dense network within the composite matrix to enhance both mechanical and electrical properties. However, this functional filler is generally outdone by its alternatives due to its sensibly higher percolation threshold (7.22–11.4 vol.%).[41] Furthermore, it generally causes the final concrete product to have lower tensile strength compared to CFs.

Other less common options include lead-zirconate-titanate nanoscale powder (nano PZT),[49] polyvinyl alcohol fibers (PVA),[50] and others; a comprehensive list is reported in Reference 51. To summarize, the two main categories—according to the filler shape—are fibrous and particle materials. According to their size, they can be catalogued as either nano-, micro-, or macro-scale.

Importantly, these conductive fillers are often combined among themselves and/or with other admixtures to improve their characteristics; for example, Reference 41 experimented with different fractions of CFs and MWCNTs[52]; produced a CB/polyethene terephthalate (PET) composite with a percolation critical value as low as 0.58 wt.%[53]; used a mixture of CFs and CB. Among other alternatives, hybrid solutions such as graphene-coated or nickel-coated CFs have been proposed as well.[54]

For direct comparability, the main properties of SFs, CFs, and the two main typologies of CNTs—as retrieved from the published scientific literature—are reported side-by-side in Table 1.

Table 2 compares different fiber-based and nanotube-based conductive fillers that, according to this review work, have been most frequently incorporated into the concrete mix for ISSC. Finally, Figure 1 portrays some examples of ISSC fillers seen at the micro- and nano-scale.

For NISSC, several embeddable sensing technologies and devices can be employed, such as fiber optic sensors (FOSs), piezoelectric sensors-transducers (PZTs), magnetostrictive sensors (MSs), acoustic emission (AE) sensors, and electrical resistance strain gauges (SGs). These are all well-known sensing devices; to recapitulate them in brief:

- FOSs can be attached to (on the surface) or embedded in the concrete to provide sensing capability. The most common types are FBG sensors, one of the most frequently used sensors in civil engineering because of their advantages such as small dimensions, accuracy, and diffuse sensing capabilities. Several categories of FOSs are available for Smart Concrete; a dedicated discussion can be found in Reference 75. FOSs can be incorporated into concrete structures to get precise strain measurements in structures to extract information regarding cracks and micro-failures. Furthermore, they can detect strain changes within seconds, which makes them suitable for dynamic signal measurements[20] and real-time monitoring.
- PZTs rely on the piezoelectric effect. For this phenomenon to occur, a solid object must have stored energy, which causes internal polarization. As a

TABLE 1 Comparative properties of steel fibers, carbon fibers, and carbon nanotubes (multi-walled and single-walled).

Property	SFs[39,55,56]	CFs[40]	Property	MWCNT[42]	SWCNT[57–59]
Fiber outer diameter (μm)	∼200–1000 e.g., 60 in.[39]	∼10-20 e.g., 15 ± 3 in.[40]	Fiber outer diameter (nm)	∼10–15	∼0.75–2
Length of fiber (mm)	∼1–10 e.g., 5 in.[39]	∼1–50 e.g., 5 in.[40]	Fiber length (μm)	∼0.1–10	Up to 30
Uniaxial tensile strength (MPa)	∼ 400–2000 e.g., 970 in.[39]	∼ 600–5000 e.g., 690 in.[40]	Uniaxial tensile strength (GPa)	∼150	∼50–500
Axial Young's modulus (GPa)	∼200	∼40–600 e.g., 48 in.[40]	Axial Young modulus (TPa)	>1	∼1
Electrical resistivity (Ωm)	$\sim 10^{-7}$–10^{-6} e.g., 6×10^{-7} in.[39]	$\sim 10^{-5}$–10^{-2} e.g., 3×10^{-5} in.[40]	Electrical resistivity (Ωm)	Up to 1×10^{-7}	Up to 1×10^{-8}
Density (kg/m^3)	∼7700–7850	∼1600–2000	Density (kg/m^3)	∼50–150	Theoretically 300–4500

Abbreviations: CFs, carbon fibers; MWCNT, multi-walled carbon nanotube; SFs, steel fibers; SWCNT, single-walled carbon nanotube.

TABLE 2 Comparison of different fiber- and nanotube-based fillers.

Conductive material	Geometric shape	Percolation threshold (vol.%)	Amount of fibers/nanotubes/nanofibers (wt.%)	References
Steel fiber (straight and twisted)	Fiber (micro)	∼0.25–2.00 (generally higher for twisted SFs and lower for straight SFs)	∼0.3–1.00 for straight SFs, 0.5–1.50 for twisted SFs	39,60,61
MWCNTs	Nanotube (nano)	∼0.30–0.70	∼0.01–0.75	42,62–64
Carbon nanofibers (CNFs)	Nanofiber (micro)	∼0.5–1.0	∼0.2–0.5	65–68

Abbreviation: MWCNTs, multi-walled carbon nanotubes.

result, two separate phenomena are deduced. When mechanical strain is applied, a change in internal polarization causes surface charge to be generated. This process is known as the direct effect and is employed for sensing. On the other hand, mechanical strain can be brought on by an applied electric field, which results in the inverse effect, used for actuation. However, as already mentioned, PZT actuators are of limited use apart from very thin, lightweight, and flexible metallic structures. Conversely, piezo impedance-based sensing can be applied to measure not only mechanical but also different parameters, including pressure, temperature, and other environmental effects. Yet, due to the superposition of these different phenomena, the same environmental factors can badly affect the strain-sensing capability of PZT sensors.[76] Embedded PZT sensors have been also widely applied for curing monitoring after concrete casting.[77] Noteworthy, PZT—lead zirconate titanate—is not the only piezoelectric ceramic, even if it is the most common one. Other alternatives, such as barium titanate, can also be applied.

- MSs are based on the magnetostrictive effect of ferromagnetic materials. That means they undergo mechanical deformation when subjected to a magnetic field. On the other hand, for sensing purposes, the inverse magnetostrictive effect refers to the phenomenon where the magnetic induction of the material changes in response to mechanical deformation. MSs, due to their capability to generate different guided wave modes by altering coil or magnet geometry, offer significant potential for long-distance inspections. However, it is important to note that the applicability of MSs is limited to ferromagnetic materials—such as rebars but not other concrete components. Also, MSs transmits relatively low ultrasonic energy with a low signal-to-noise ratio, and the induced energy is critically dependent on the location of the probe with respect to the damaged component.
- The detection principle of AE sensors is based on the acoustic emissions (waves) generated by microcracking into the concrete volume in response to deformation and/or crack growth when internal stresses locally exceed the material resistance at a microscopic

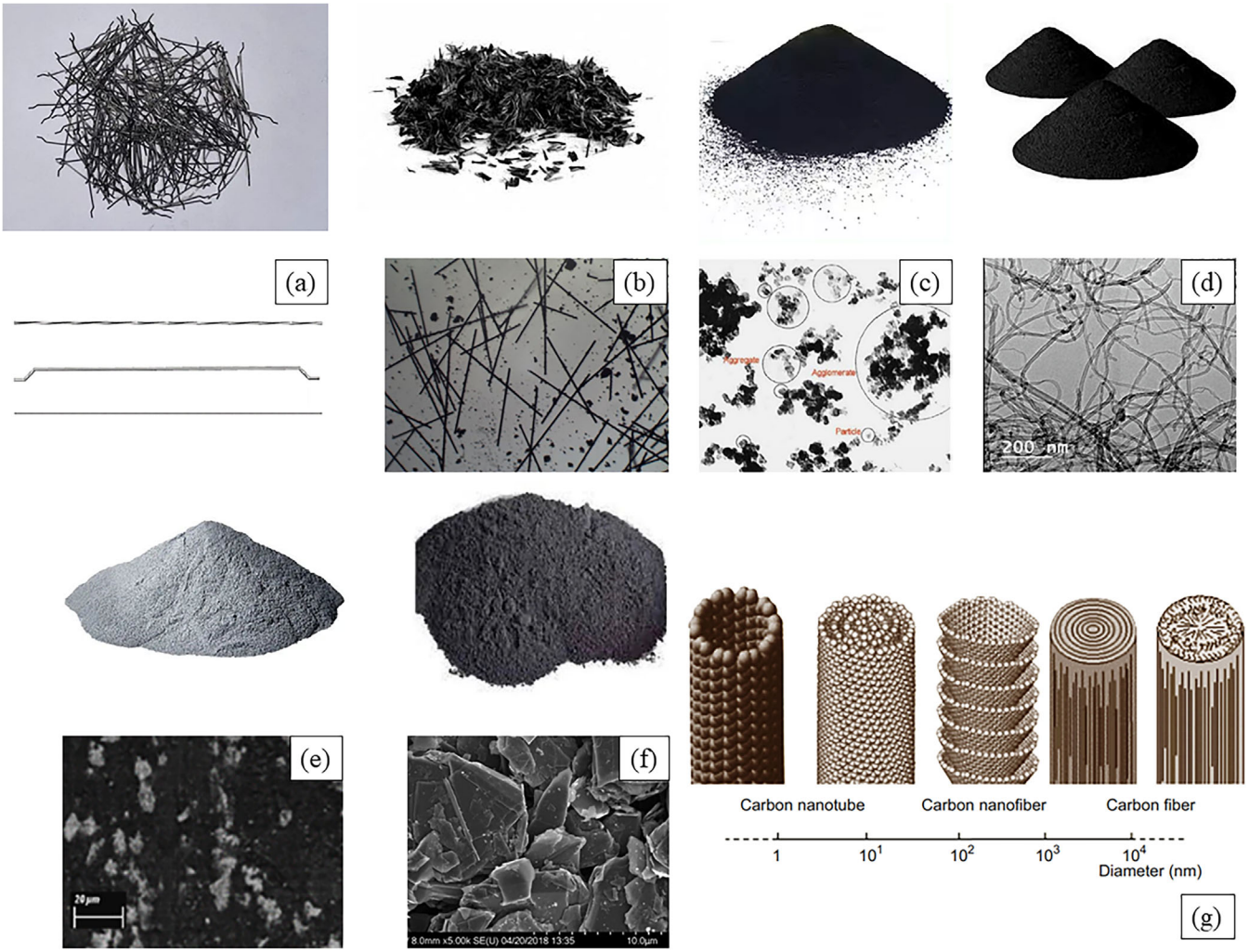

FIGURE 1 The most common conductive fillers and ISSC solutions according to this review. (a) Steel fibers (above: example of 50-mm long hooked-end SFs; below: single specimen of twisted, hooked-end, and straight SFs, retrieved from Reference 69). (b) Carbon fibers (above: macro-scale view; below: micro-scale view of CFs, retrieved from Reference 70). (c) Carbon black (above: macro-scale view; below: micro-scale view of CB particles, retrieved from Reference 71). (d) Carbon nanotubes (above: macro-scale view; below: nano-scale view of CNBs, retrieved from Reference 72). (e) Nickel powder (above: macro-scale view; below: micro-scale view of NP particles, retrieved from Reference 44). (f) Nanoscale graphite powder (above: macro-scale view; below: micro-scale view of nanoscale GP particles, retrieved from Reference 73). (g) Schematic comparison of the diameter dimensions on a log scale for various types of carbon-based nanotube and nanofiber variants, retrieved from Reference 74. CB/CNB, carbon black; CFs, carbon fibers; GP, graphite powder; ISSC, intrinsically self-sensing concrete; NP, nickel powder; SFs, steel fibers.

scale. AE sensors are conventionally made of bulky piezoelectric materials such as the aforementioned PZT. As stated before, they convert the mechanical energy of the acoustic emissions into electrical signals, which can then be processed and analyzed, using different technologies and operating at different frequency scales. In the context of NISSC, these sensors are embedded within the concrete during its construction. However, due to the very limited range of detectability, the use of AE sensors is hampered by practical and economic considerations.

- Electrical resistance SGs are, arguably, the most widely used sensors for NISSC, due to their historic use in non-embedded SHM, ease of installation, durability, and very low cost. The functionality of SGs is simple and reliable: once set under a continuous electrical current, if a force or deformation is applied to the sensor, the electrical resistance changes. By detecting these resistance changes, it is possible to indirectly measure the strain of the concrete where the sensor is embedded (or attached). They are only able to sense strain and not other

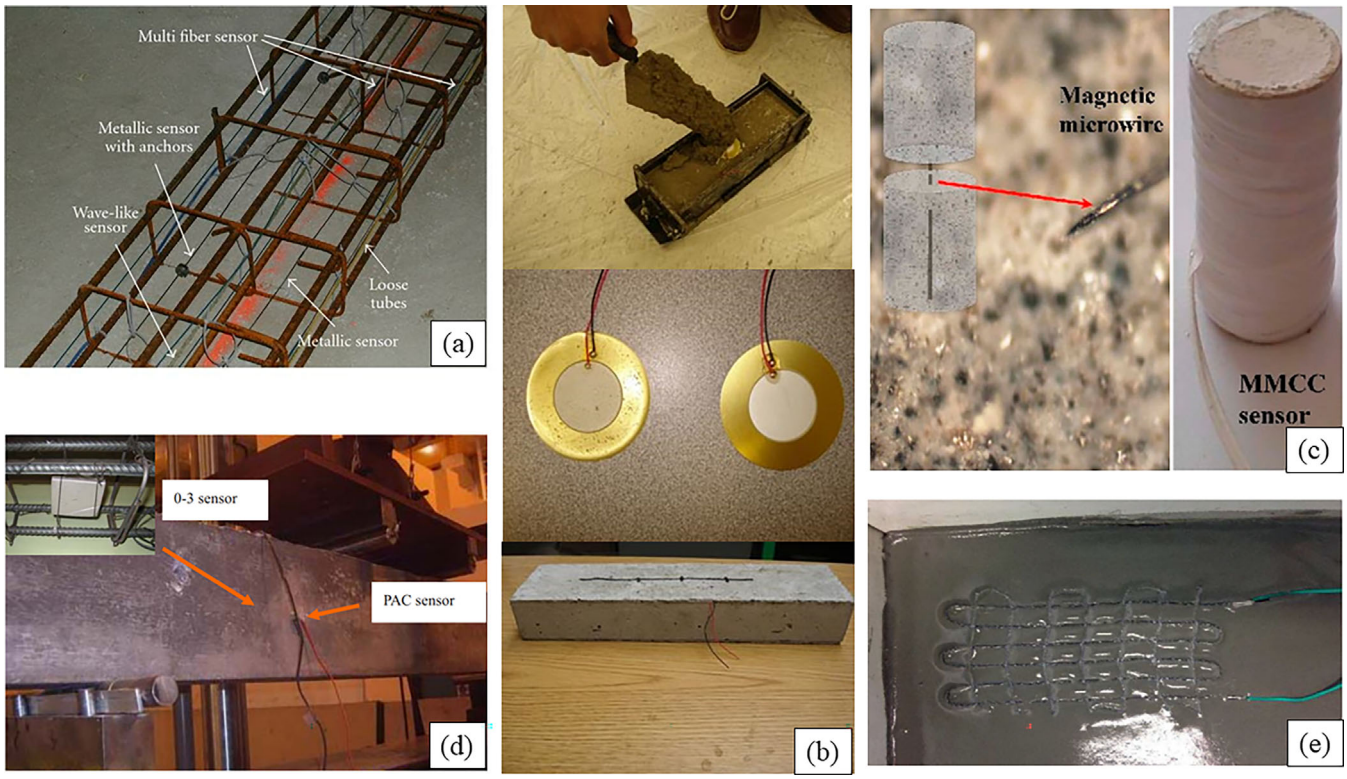

FIGURE 2 Summary of the most common NISSC alternatives according to this review. (a) Concrete-embedded FOS, attached to the rebars before concrete casting (retrieved from Reference 82). (b) PZT sensors; from top to bottom: embedment, piezoelectric disks covered with a protective layer of rubber, and final specimen after curing (retrieved from Reference 83). (c) MS sensor (microwire of ferromagnetic material) embedded in a cylindrical specimen (adapted from Reference 84). (d) Piezoelectric sensors for AE sensing before and after embedment in an RC beam specimen (retrieved from Reference 85). (e) Prototype strain gauge during embedment in concrete (retrieved from Reference 86). AE, acoustic emission; FOS, fiber optic sensor; MS, magnetostrictive sensor; NISSC, non-intrinsic self-sensing concrete; PZT, lead-zirconate-titanate; RC, reinforced concrete.

parameters like moisture or temperature. On the other hand, they are not affected by these damage-unrelated factors. Yet, they are sensitive to electromagnetic interference.

A few selected examples are depicted in Figure 2. Another less common but still noteworthy application regards concrete-embedded MEMs barometric pressure sensors for strain measurement,[78,79] proposed for the monitoring of concrete tunnel linings.[80]

Finally, another relevant technology is passive radio frequency identification (RFID), which is not intended for sensing but rather enables short-distance passive wireless communications between the sensors and a receiving station. This allows for data transmission from fully embedded NISSC sensors to the outside.[81]

In conclusion of this introductive part, Table 3 provides a brief comparative view of the main ISSC and NISSC solutions based on this review's findings.

2.2 | Key aspects of ISSC technology

As mentioned before, the focus of this work is on ISSC. Therefore, it is further required to highlight the following points:

2.2.1 | Fiber dispersion and mix preparation

To properly activate the self-sensing properties of concrete, the process of dispersion of micro- and nano-fibers in the composite mix must achieve a homogeneous distribution of the functional filler within the cement matrix. As mentioned, that will establish a conductive network, reducing the resistivity of the nonconductive matrix at the macroscale. Some conductive fillers, such as, CNTs, have a natural tendency to agglomerate because of their large surface area, high aspect ratio, and strong Van der Waals forces. Due to this issue, without proper countermeasures, the dispersion is limited and thus reduces the

TABLE 3 Comparison of ISSC versus non-ISSC solutions.

Material	Type	Sensing capability	Advantages	Disadvantages
Carbon fibers (CFs)	ISSC	• Monitors mechanical strain and damage within concrete	• May improve mechanical properties	• Relatively higher cost • Limited repeatability
Carbon nanotubes (CNTs)	ISSC	• Detects changes in electrical conductivity due to strain or damage	• Enhanced electrical conductivity	• Challenging dispersion • Costly production • Moderate repeatability
Graphite powder (GP)	ISSC	• Measures electrical resistance changes in response to strain or damage	• Excellent electrical conductivity	• Challenging dispersion • Costly production • Moderate repeatability
Carbon black (CB)	ISSC	• Detects changes in electrical properties due to strain or damage	• Enhanced self-sensing behavior • Relatively low cost	• May affect the workability of fresh concrete • Cost considerations • Moderate repeatability
Nanoscale graphite powder (GP)	ISSC	• Utilizes nanomaterials to enhance self-sensing properties	• Improved sensitivity and accuracy	• High research and development costs • Material availability • Moderate repeatability
Fiber optic sensors (FOSs)	NISSC	• Measures strain through changes in light intensity within optical fibers	• High sensitivity. External monitoring • High repeatability	• Installation complexity • Cost of sensors
Electrical resistance strain gauges (SGs)	NISSC	• Monitors electrical resistance changes due to strain	• Easy installation • Real-time strain monitoring • Very low cost • High repeatability	• Sensitive to environmental conditions • Requires external wiring
Piezoelectric materials (PZT)	NISSC	• Converts mechanical stress to electrical signals for strain detection	• Suitable for dynamic monitoring • Moderate costs	• Limited sensitivity • May require protective coatings • Moderate repeatability
Acoustic emission (AE) sensors	NISSC	• Detects microcracks and damage through acoustic waves generated during fracture	• Enables real-time monitoring • Detects hidden damage	• Requires external power supply • Requires specialized equipment • Interpretation of signals can be complex • Relatively high costs • Moderate repeatability
Magnetostrictive sensors (MSs)	NISSC	• Measures strain through changes in magnetic properties	• Durable and reliable • Moderate costs • High repeatability	• Requires external power supply

Note: Based on Reference 87 and Reference 88.
Abbreviation: ISSC, intrinsically self-sensing concrete; NISSC, non-intrinsically self-sensing concrete.

effectiveness of the CNTs when used in the composite mix.[89] These countermeasures can be either physical or chemical depending on their working principle. Physical methods include sonication, ball milling, and mechanical stirring; these limit CNT and fiber agglomerates by providing mechanical energy to overcome Van der Waals interactions. In particular, sonication tends to reduce the agglomeration of the fibers by generating pressure waves at high speeds. Ball milling and mechanical stirring (also using magnetic stirrers) are not considered very effective on their own[22] and thus generally only used along with sonication for more effective dispersion.

TABLE 4 Main dispersing materials and respective dispersed fillers.

Type	Dispersing material/surfactant	Dispersed functional filler	References
Surfactant	Water-reducing agent	CF, CNT, CNF, CB, GP, NP	[91,92]
	Methylcellulose (MC)	CF, CNT	
	Carboxy MC	CF	
	Sodium dodecyl sulfate (SDS)	CNT, CNF	
	Polystyrene sulfonate (PSS) + N-methyl-2-pyrrolidone (NMP)	CNT	
	Dodecyl-benzene sodium sulfonate (NaDDBS)	CNT	
Mineral admixtures	Fly ash	CF, CB, SF, NP	[92]
	Silica fume	SF	[93,94]

Abbreviations: CB, carbon black; CF, carbon fiber; CNF, carbon nanofiber; CNT, carbon nanotube; GP, graphite powder; NP, nickel powder; SF, steel fibers.

The second typology of methods relies on chemical reactions to improve the dispersion process. This is made possible through the addition of several oxygen groups, such as carboxyl (COOH) groups, to form covalent bonds or by growing polymer chains from the CNT surfaces. The use of surfactants—such as plasticizers—is also common to disperse the functional fillers, using electrostatic repulsion between the fibers and increasing aqueous solubility. In this case, a solvent, made of a proportion of water and surfactant, is used. In the case of CNTs, they adhere to the hydrophobic part of the surfactant via Van der Waals forces, while electrostatic repulsion ensures their distribution. The optimal quantities of both surfactants and CNTs can be found by experimentation and trial and error and depend on the type of surfactant used. Superplasticizers are also used due to their compatibility with cement and are necessary for MWCNTs due to their high specific surface area.[90] In all cases, several mix preparation methodologies—most commonly classified as first, synchronous, and latter admixing methods[87]—are used, depending on the chemical dispersant and the mechanical mixing procedure. Table 4 reports a brief description of the different dispersing materials found in this review work.

The combined usage of mechanical and chemical methods, such as sonication coupled with the addition of surfactants, can effectively increase the phenomenon of fiber and CNT dispersion.[89,90]

2.2.2 | Sensing techniques

Sensing within Smart Concrete materials is done through two most prominent methods: two- or four-probe electrode configurations. Both consist of the application of a current I and the measurement of a voltage V. However, they differ in the number of electrodes applied.[92,95] This and other main differences reported by the works reviewed here are summarized in Table 5. In a few words, the two-probe configuration is a more straightforward setup, suitable for simple and expedited resistance measurements, but generally regarded as not accurate for self-sensing applications.[32,96] Conversely, the four-probe configuration is preferred, as—for a slightly less complex setup—it can return more accurate and reliable measurements of the changes undergone by the electrical resistance in the concrete's specimens under applied deformations or loads.[87,97] Due to contact resistance between electrodes and the piezoresistive cement-based material, the two-probe and four-probe readings will not be identical, with an apparent higher resistance measured in the two-probe configuration.

Besides resistance measurement, the electrode material, serving as a conduit between the cement composite and the measuring elements, assumes critical importance. The electrode should exhibit low electrical resistance and stable electrical conductivity. Various metals, including copper, stainless steel, silver, and aluminum, are utilized as electrodes in forms such as metal plates with or without holes, metal foils, meshes, bars, and copper wires coated with conductive paints like silver, copper, and carbon black (Figure 3).

As mentioned earlier, two measurement methods, DC and AC, are commonly used. The DC test method, which is considered the simplest option among the two, has its limitations as the current does not propagate over larger areas, which induces ion movement and results in electrical polarization within the composite. This electrical polarization limits the measurement of electrical resistance and thus is a great concern. To avoid this, a DC voltage is applied to the composite prior to loading, which ensures polarization completion at the time of measurement. An alternative approach involves the use of AC, where polarization still occurs but can be dealt with by expanding the frequency range and reducing the amplitude of the AC voltage.[98–102]

TABLE 5 Key distinctions between two- and four-probe setups for ISSC.

	Two-probe configuration	Four-probe configuration
Easiness of measurement setup	• As only two electrodes are required, it is inherently simpler, faster, and more cost-effective to implement.	• It is relatively more complex and expensive to implement because it requires four electrodes, two for the current application and two for the voltage measurement.
Contact resistance	• As the current and voltage are measured through the same electrodes, the contact resistance between the electrodes and the concrete sample affects the measured electrical resistance.	• As the current is applied through two electrodes, while the voltage is measured through two separate electrodes, the effect of contact resistance is minimized.
Sensing coverage, spatial resolution, and sensitivity to heterogeneity	• Can provide accurate measurements for the specific points between the probes. However, it may lack precision in assessing the overall material properties outside of it. Thus, it is suitable for applications where localized information is sufficient. • Due to its localized sensing coverage and lower spatial resolution, it may struggle to detect subtle localized variations or heterogeneities within the concrete.	• Can offer higher accuracy and precision in determining material properties across a larger area. As it measures properties across multiple points, it can offer higher spatial resolution, thus allowing for a finer analysis of variations in material properties within the concrete. • Due to its larger coverage and better spatial resolution, it is more adaptable to localizing heterogeneities and/or discontinuities (damage localization).
Accuracy	• Less accurate voltage measurements due to the superposition of contact resistance and concrete sample resistance in the measured quantity.	• More accurate voltage measurements due to the missing effects of contact resistance.
References	32,87,96	32,87,97

Abbreviation: ISSC, intrinsically self-sensing concrete.

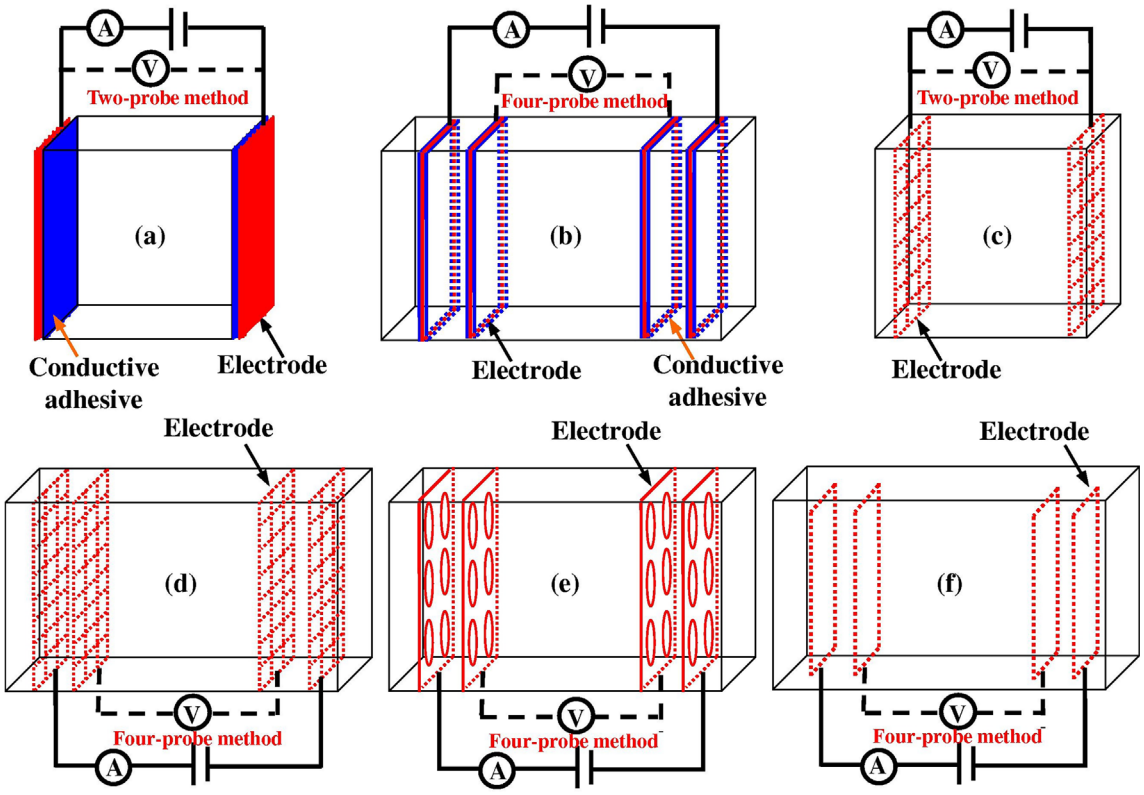

FIGURE 3 Two (a and c) and four (b and d–f) probe configurations. (a and b) Electrodes attached on the surface. (c–f) Embedded mesh, perforated plate, and loop electrode configurations. Retrieved from Reference 23.

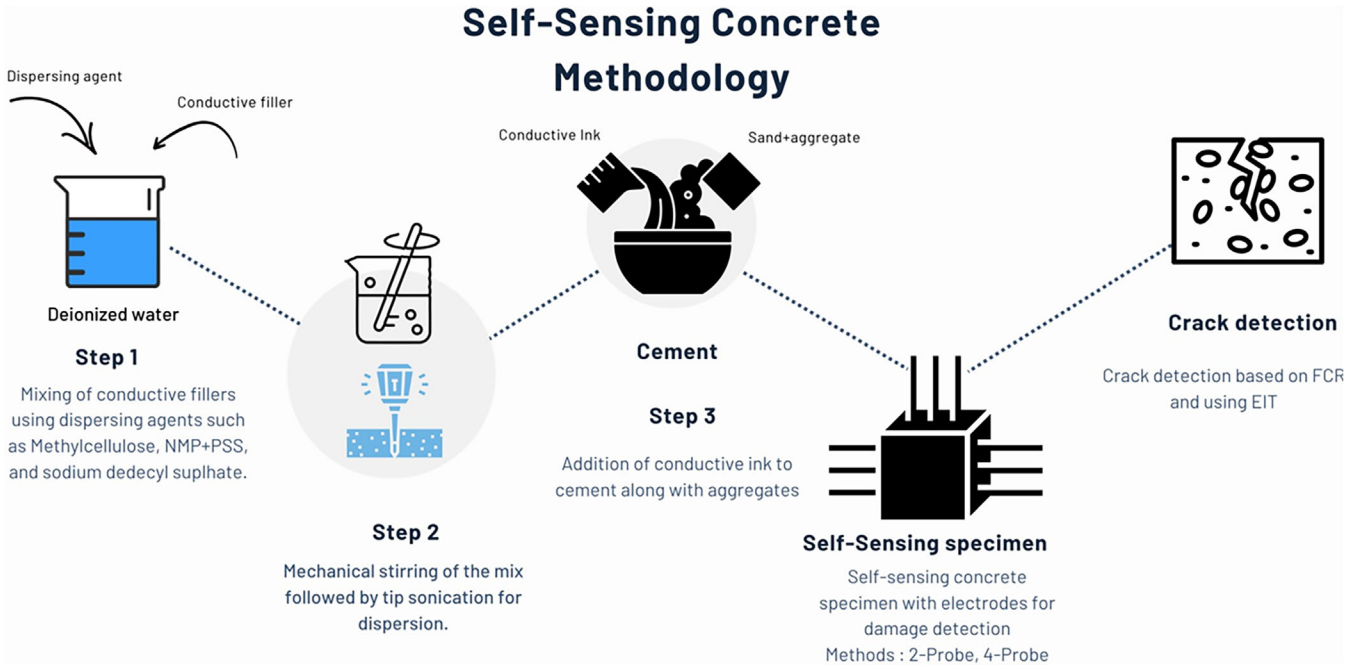

FIGURE 4 Main steps of ISSC preparation and application for damage detection. EIT, electrical impedance tomography; FCR, fractional change in (longitudinal) electrical resistivity; ISSC, intrinsically self-sensing concrete; NMP, N-methyl-2-pyrrolidone; PSS, polystyrene sulfonate.

To conclude this section, Figure 4 conceptually depicts the several steps involved in the ISSC preparation, implementation, and application methodology, including mix preparation and probe sensing.

3 | EXEMPLARY LABORATORY-TESTED APPLICATIONS OF SSC

Hereinafter, a few examples of the most interesting recent applications encountered in the literature are proposed, to highlight several potential uses of Smart Concrete, even for unconventional and/or nonstructural purposes.

3.1 | Nano-engineered SSC for crack detection and propagation

In References 103 and 104, the authors introduced a new strategy for damage detection and assessment using nano-engineered concrete in which a conductive ink is sprayed onto the aggregates instead of mixing the conductive materials within the composite mix. Generally, in a concrete mix, fine and coarse aggregates are carefully distributed to form a dense structure for high compressive strength, as aggregates primarily bear the load transfer in concrete. Since the aggregates are already distributed within the mix spraying these aggregates creates a dense conductive network, with the cement matrix playing a crucial role in bonding the aggregates.

80 × 80 × 20 mm cubic specimens were produced, using conventional concrete, aggregate-coated conductive concrete, sand-coated conductive concrete, and a mix of sand- and aggregate-coated. The conductive coating consisted of a latex polymer containing a specific quantity of multi-walled CNTs. Incorporating MWCNTs into highly viscous polymers can be achieved through emulsion polymerization methods, such as with polystyrene (PS) or polymethylmethacrylate (PMMA). In this case, MWCNTs were dispersed in an aqueous solution through ultrasonication before adding the latex polymer to create an MWCNT-latex ink. This highly conductive ink was then sprayed onto fine and coarse aggregates to ensure uniform distribution and achieve a coating thickness of a few microns (Figure 5a,b). After drying, the coated aggregates were directly incorporated into the concrete mix. The main difference and supposed advantage of incorporating a conductive interphase into concrete aggregates is the direct creation of a conductive concrete rather than an indirect formation through the intermediate step of a conductive cement paste. According to the authors, conductive cement paste containing fine and coarse aggregates aimed to create conductive concrete might not yield the expected or required results due to inadequate CNT distribution for forming a conductive network. By

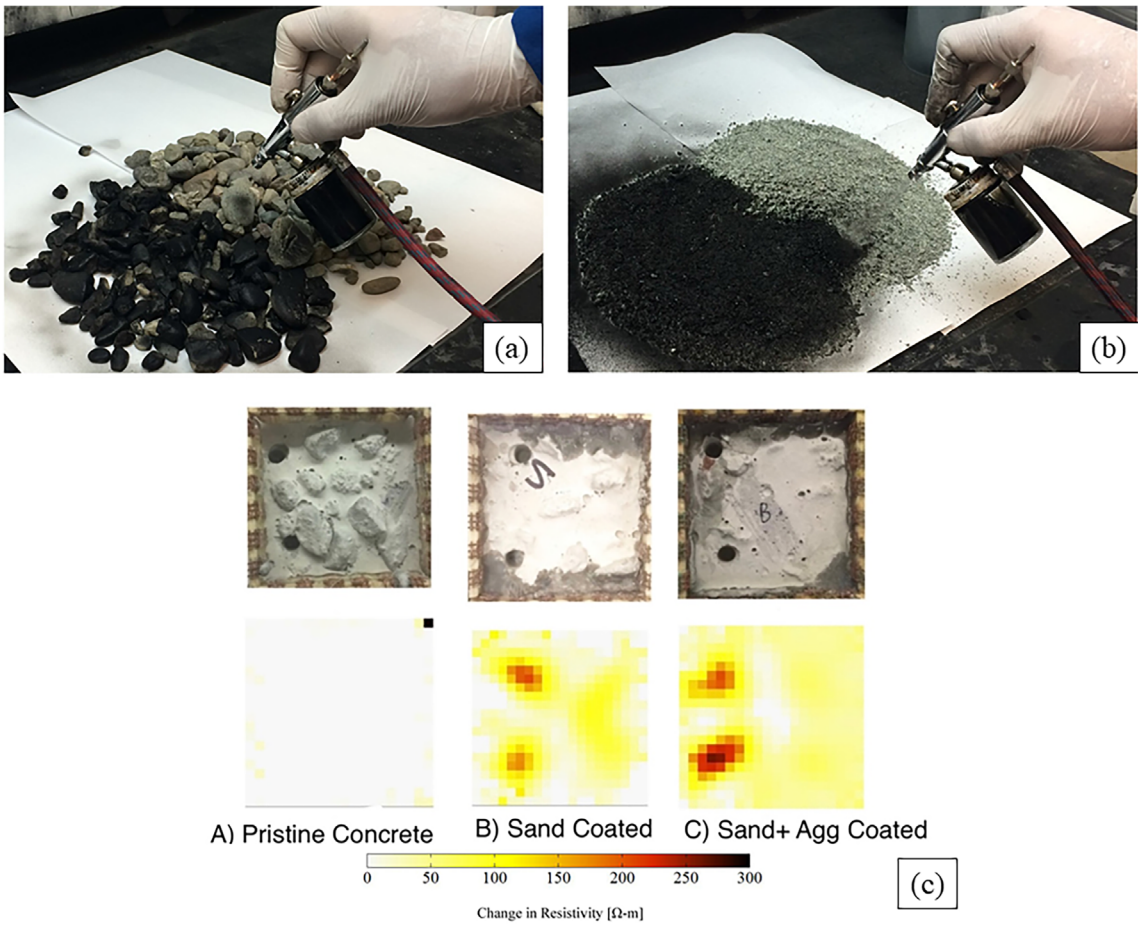

FIGURE 5 (a and b) Airbrushing coarse and fine (sand) aggregate to get nano-engineered self-sensing concrete. (c) Spatial damage detection through EIC mapping for different samples with conventional concrete (A), MWCNT-coated fine aggregate (B), and MWCNT-coated fine and coarse aggregate (C). Adapted from Reference 103.

establishing a conductive interphase around concrete aggregates, a better conductive network could be formed. This would offer more efficient and sensitive measurements as compared to other self-sensing cementitious composites. Furthermore, the development of conductive concrete offers new possibilities for strain sensing and damage detection systems. Unlike cement-based sensors requiring embedding at multiple locations within a structural element, a large portion of the element can be made conductive with coated aggregates. This would potentially enable the monitoring of any part of the structure, even if, from a practical point of view, spraying all aggregates will be too costly and too challenging with the current industrial processes.

It should be noted that electrical conductivity varies depending on the volume fraction of MWCNTs. While MWCNTs exhibit excellent material properties for strain sensing, such as high electrical resistivity, latex has inherently low mechanical and electrical properties, such as tensile strength and electrical conductivity, respectively.

The results of this study were evaluated in terms of electrical impedance tomography (EIT) imaging. EIT is a method that involves the placement of electrodes around a structural element to enable the current flow. A low-magnitude AC is then used as an input between a pair of boundary electrodes, while voltage is measured at the remaining electrodes. Thus, voltage and phase measurements are recorded in such a way. This is then used to acquire the complete set of boundary voltage responses. These measured voltage responses are used to address the EIT inverse problem and reconstruct the spatial impedance distribution. With these settings, EIT enables strain sensing and, as a consequence, damage detection and localization, by creating a resistivity map of the entire region under investigation. EIT mapping, especially resorting to the difference between images taken at different times, has been applied for moisture propagation tracking,[105] therefore approximating the position of water inside concrete specimens[106] and its total content.[107]

For damage detection, macroscopic holes were drilled into conventional and enhanced concrete specimens (see Figure 5c). No prominent changes in resistivity distributions were observed in the reconstructed resistivity profiles of the conventional concrete plates. This insensitivity to damage could be attributed to the high resistivity of pristine concrete, impeding adequate electrical current propagation. Consequently, the measured boundary voltage responses did not reflect damage features resulting from hole drilling. Similar experiments were conducted on concrete cast using large aggregates coated with the MWNT-latex thin films. They yielded comparably unsuccessful damage detection outcomes. Conversely, resistivity maps from EIT testing on sand-coated and sand-plus-aggregate-coated specimens clearly detect and localize the position of the drilled holes. That is largely due to the higher conductivity; in turn, this enhancement can be attributed to the increased presence of conductive cement–aggregate interfaces.

In terms of mechanical properties, the compressive and flexural strengths of the Smart Concrete solution were evaluated and benchmarked with conventional concrete. The lowest average compressive strength was observed in the aggregate-coated mix, which nevertheless satisfied the required strength of 4400 psi under the provided guidelines. A sand-coated mix and both sand- and aggregate-coated specimens resulted in an average compressive strength of 6860 and 7580 psi, respectively. Meanwhile, specimens of conventional concrete reached an average strength of 7030 psi. These findings suggest that the mechanical properties of concrete can be maintained when cement–aggregate interfaces are modified with MWNT-latex thin films. More specifically, sand-coated specimens achieved comparable, if not superior, compressive strengths to conventional concrete. Nevertheless, coating the large aggregates compromised their mechanical properties. While this may be perceived as a drawback of modifying the cement–aggregate interface with MWNT-latex thin films, the authors stated that their primary goal was to meet or exceed design guidelines rather than preserving the material properties of concrete unchanged. In contrast, coating sand did not appear to produce negative effects, likely attributed to its smaller particle size and intrinsic jagged surface. The modulus of rupture followed a quite different trend, with the highest value among nonconventional concretes reached by the aggregate-coated solution (950 psi w.r.t. 953 psi of pristine concrete). The lowest value (821 psi) occurred in the combined sand-plus-aggregate-coated case.

In terms of cost comparison with conventional RC, considering the average price of concrete at approximately US\$122/m^3, a significant cost increase was evident when CNTs were directly dispersed within the cement matrix. For example, concrete with 0.5 wt.% of MWNTs incurred a 52-fold increase in costs compared to pristine concrete. On the other hand, sand-coated specimens have substantially lower cost. The reduced cost associated with modifying cement–aggregate interfaces implies that this technique can be used for practical applications of the material. It is worth noting that the specimens in the study were not optimized for sensing and mechanical performance, suggesting the potential for further cost reductions.

3.2 | Temperature and hydration monitoring

In their recent publication, the authors of Reference 108 proposed CNF-incorporated "SmartCem" sensors, that is, a nanomodified Portland cement, for the monitoring of RC internal temperature and moisture content. The rationale is that the formation of a uniform cementitious matrix depends on the process of cement hydration. Thus, temperature and hydration monitoring inside the concrete itself can be used to extract information about its current and future performances.

The so-called SmartCem sensors (Figure 6a) were developed by synthesizing CNFs on Portland cement particles through the chemical vapor deposition (CVD) process. Different proportions of nanomodified cement were used to create mortars for sensor fabrication, to study the range of sensor amount used to monitor hydration and temperature processes, up to 2.71 wt.%; 12 × 12 × 60 mm SmartCem prisms were inserted into 100 × 100 × 100 mm cubic normal-strength concrete samples (Figure 6b).

Using a digital multi-meter and a four-probe technique, the electrical resistance of the SmartCem sensors was measured at −20, +20, and +40°C for temperature monitoring. The temperature coefficient and activation energy were determined by applying direct current to the outside electrodes and measuring the potential change at the inner electrodes. Similarly, the SmartCem sensors were inserted into concrete cubes just after casting to test for hydration sensitivity.

Large-scale self-compacting concrete beams were monitored for cement hydration using the proposed sensors. The sensors showed that they could monitor changes in electrical resistivity after 7 days of casting, which was in good accordance with the expected hydration processes. The use of commercially available humidity and thermocouple sensors were used for benchmarking.

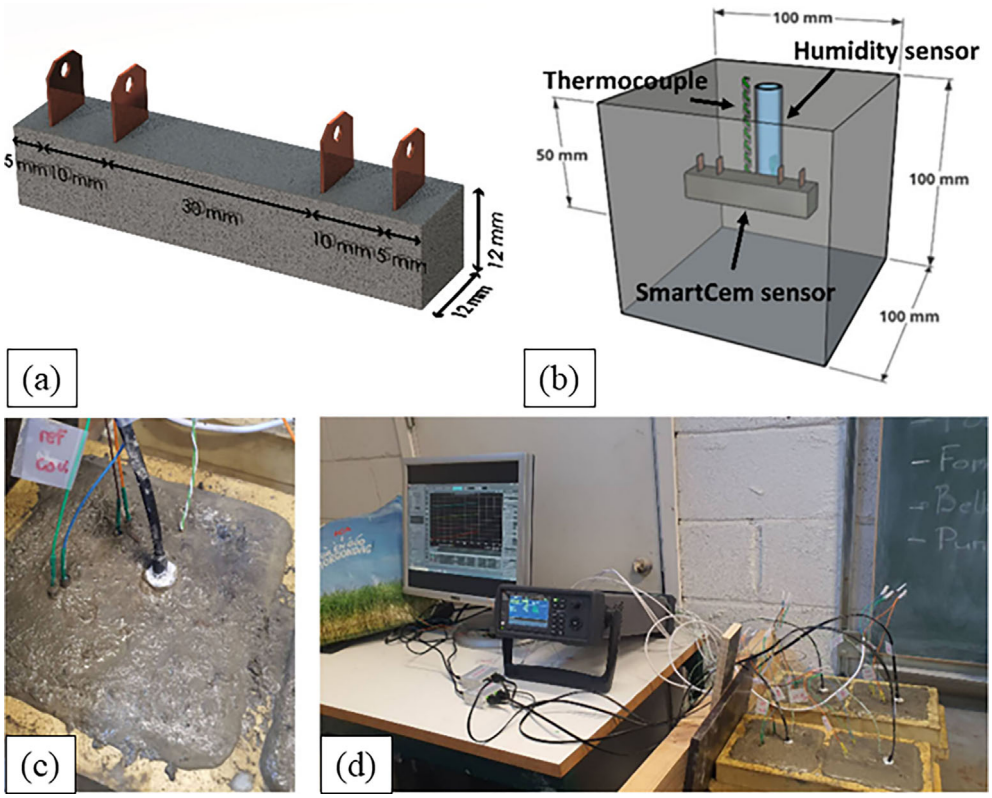

FIGURE 6 (a) Mortar sensor with electrode setup; (b–d) sensor placement and test setup for hydration monitoring. Adapted from reference 108.

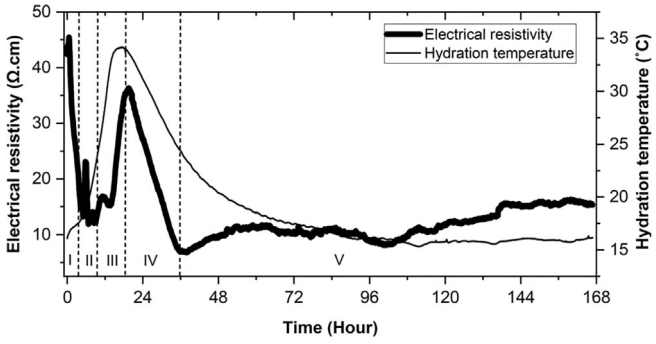

FIGURE 7 Hydration temperature trend and measurement of electrical resistivity by SmartCem sensors. Retrieved from Reference 108.

As a result, the electrical resistivity was confirmed to change following cement hydration. It was found to decrease as well following temperature increases. The sensor with the highest temperature sensitivity, with an approximate 11.76% increase over the reference sample, was the one containing 10 wt.% of SmartCem nanomodified Portland cement (which, in turn, corresponds to 0.271 wt.% CNFs). Additionally, the hydration sensitivity testing revealed that SmartCem sensors containing 4 wt.% of binder exhibited a resistivity change that followed the kinetics of cement hydration, showcasing their hydration sensitivity (see Figure 7).

3.3 | UHP SSC

In Reference 109, the self-sensing capabilities of UHSC were investigated. The rationale is that fiber-reinforced solutions are already incorporated in UHSCs—both with and without traditional rebars.[110,111] Hence, the same SFs can be exploited for the additional aim of self-sensing. In this case, straight brass-coated SFs with high tensile strength (2300 MPa), relatively high length (13 mm), and low diameter (60 μm) were used in combination with ASTM Type I normal Portland cement, polycarboxylate-based superplasticizer, and undensified silica fume. The fibers amounted to 0.5 vol.% of the cement paste. Three 50-mm cube specimens were cast for compressive strength testing, and three 40 × 40 × 160 mm prism specimens were cast to determine the electrical resistivity and piezoresistivity (via four-probe testing). All specimens were cured for 28 days. To differentiate specimens with different moisture conditions, oven-drying (60°C and 20% humidity) and air-drying were used. Finally, a UHSC column was realized, embedding the oven-dried specimens (Figure 8a,b).

From cyclic compression tests, it was evidenced that for all specimens, the expected general trend of the piezoresistive behavior was confirmed, with FCR decreasing upon loading, corresponding to the

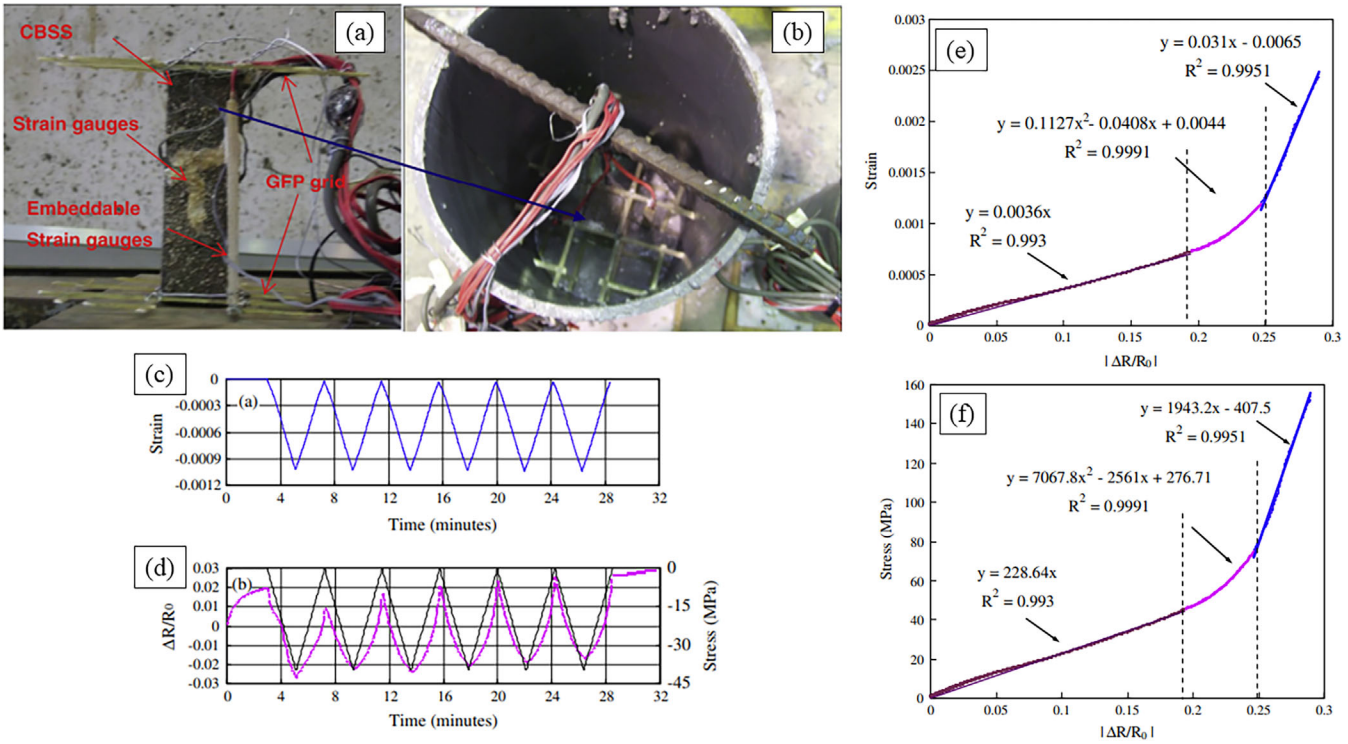

FIGURE 8 (a and b) Self-sensing specimen and its embedding into a UHSC column. (c and d) Strain (blue line), stress (black line), and FCR (purple points) experimental curves for one air-dried specimen during the cyclic load test. (e and f) Direct relationships between the fractional change in resistance and strain and between FCR and stress, as obtained from the UHSC column loaded till failure. Adapted from Reference 109. FCR, fractional change in (longitudinal) electrical resistivity; UHSC, ultra-high strength concrete.

decreasing resistance, and increasing upon unloading, corresponding to the increasing resistance. However, $\Delta\rho/\rho_0$ was subject to irreversible changes after any cycle, implying that the piezoresistivity has poor repeatability in UHSC (Figure 8c,d), as already known in regular concrete as well. Interestingly, both air- and oven-dried specimens returned comparable mechanical properties (very high compressive strength at circa 120–130 MPa, elastic modulus of circa 40–42 GPa, and Poisson's ratio 0.17), but the resistivity and GF were sensibly higher for controlled oven-dried specimens than air-dried ones ($3.34 \cdot 10^3$ vs. $1.41 \cdot 10^3$ Ωm and GF = 202 vs. 42).

The column destructive test allowed the definition of three regions in the FCR $-\varepsilon$ and FCR $-\sigma$ curves of UHSC under monotonic loading (Figure 8e,f): firstly, a highly sensitive, linear phase at low strains/stresses; then, a subsequent medium sensitive, nonlinear phase; finally, a last phase characterized again by a linear relationship but hampered by low sensitivity. The occurrence of such linear and nonlinear regimes for monotonic loading is confirmed in other research works as well, for example, by Reference 112 where both stainless SFs and copper-coated SFs were experimentally tested.

3.4 | Leakage detection

Cement with an embedded conductive filler can demonstrate great potential in sensing changes in the mechanical environment such as for leakage detection. In Reference 113, Portland cement class G was used with Pyrograf PR-19 XT-LHT CNFs (size: between 50 and 200 μm in length and about 150 nm in diameter). The cement/CNF slurry was prepared using deionized water and a superplasticizer polymer as the dispersing agent (5.2 CNF to dispersant weight ratio). Two 3 × 3 × 3 cm cubic samples were cast, with two 2 × 3 cm steel plates inserted into the slurry with a 1 cm thick separator placed between them for two-probe testing (Figure 9a). This was conducted under uniaxial compression testing (Figure 9b). ISSC readings were paired and compared to the acoustic emissions recorded by physically attached transducers (Figure 9c,d) and X-ray tomography imaging of the specimens.

As a result, the Portland G well cement with an embedded conductive filler exhibited sensitivity to mechanical load, with significant changes in electrical resistivity. This decreased in the elastic deformation region, while a notable increase in resistivity, accompanied by numerous acoustic events, was observed in the

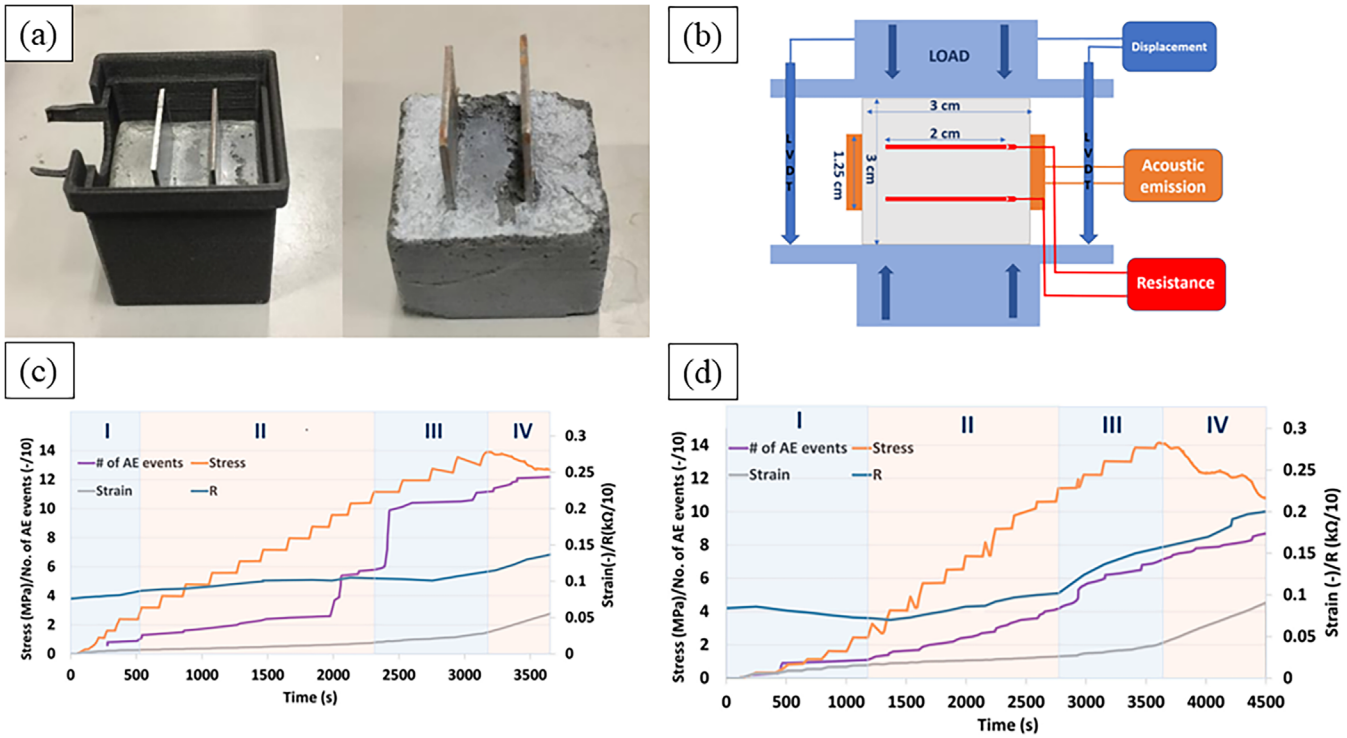

FIGURE 9 (a) Photography of one sample within and without the mold after 24 h of curing. (b) Schematic representation of the experimental setup with electrical connectors and surface-attached AE sensors. (c and d) Results from Samples 1 and 2. Adapted from Reference 113. AE, acoustic emission.

plastic deformation region. This increase further continued beyond the failure threshold, along with an increase in the number of acoustic events. Although results were qualitatively reproducible for two similar samples, the magnitudes of resistivity changes differed, attributed to the stochastic nature of fracture growth and propagation, influenced by micro-sized inhomogeneities (nanofiber aggregates). Nevertheless, it is important to note that while Portland G cement with CNFs showed promising results for detecting mechanical stress and strain, the authors did not directly test its in situ application. Also, the occurrence of leakage was not directly investigated but rather indirectly related to the occurrence of cracking inside the specimens. Nevertheless, the potential application is of great interest and future studies in this direction may benefit the whole research community.

3.5 | Other ISSC and NISSC applications

3.5.1 | Fatigue monitoring

Fatigue monitoring is of paramount importance for concrete and R.C. structures and infrastructures; however, the specific topic has been addressed only by a very limited number of scientific papers. In very recent years, self-sensing cement-based materials have been proposed and laboratory-validated by Adresi et al.[114] (using MWCNTs in 10 × 10 × 40 cm concrete specimens), Çelik et al.[115] (testing both MWCNTs and CFs in 10 × 15 × 100 cm R.C. beams), and Xu et al.[116] (using CFs and performing wheel loading in a 280 × 300 × 190 cm R.C. deck slab).

3.5.2 | Railroad applications

Regarding the specific applications to civil infrastructures, apart from road bridges, it is worth recalling that ISSC solutions have been tested on railroads as well, with interesting applications validated in situ and during operational conditions for a real high-speed railway line (Shanghai-Hangzhou, K005, China),[117] as well as field tested with controlled input conditions for a Maglev train girder under static load test.[118]

3.5.3 | Other uses of electrically conductive concrete (ECON)

Apart from self-sensing, the addition of an electrically conductive network in the concrete mix can be exploited

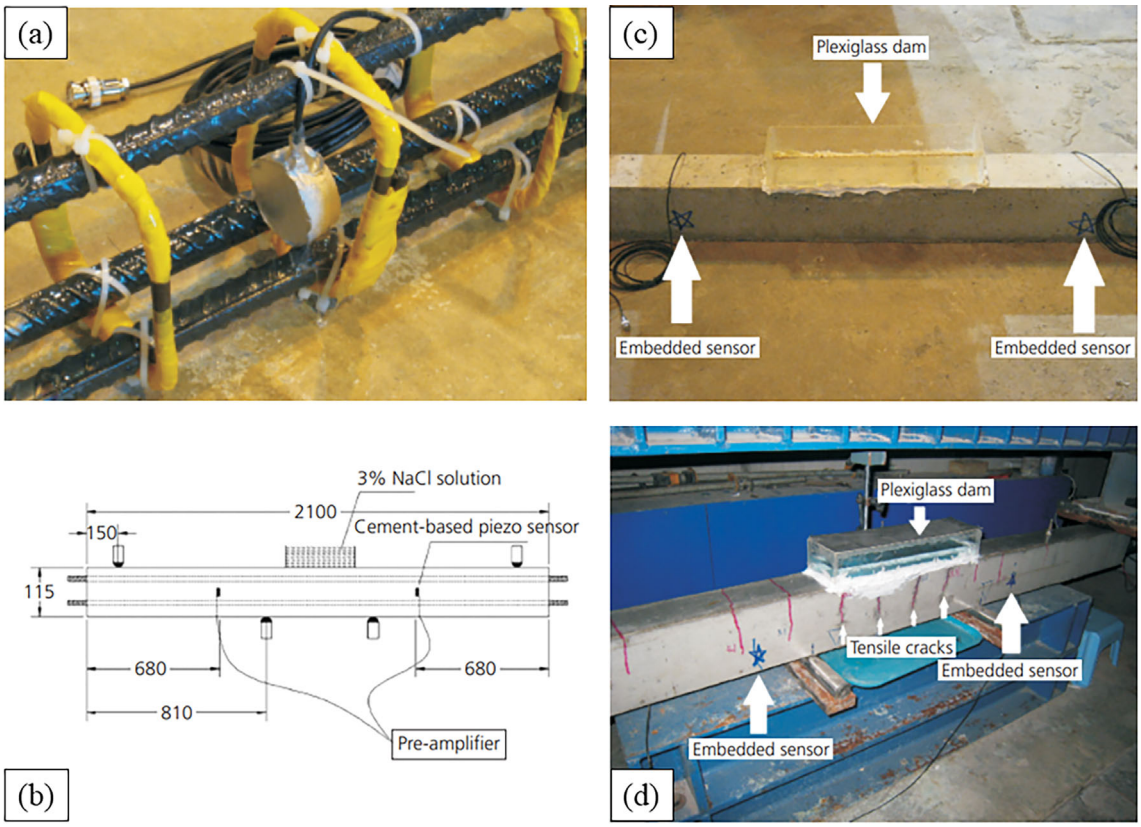

FIGURE 10 (a) Embedded cement-based piezoelectric sensor before casting. (b) Experimental setup of the wet-dry accelerated corrosion of RC beam (dimensions in mm). (c) RC beams under the effect of corrosion only. (d) RC beams under the coupled effect of loading and corrosion. Adapted from Reference 122. RC, reinforced concrete.

for secondary and additional uses, for example, for concrete-based heated pavement systems (HPS). The conventional methods for removing ice and snow from pavement involve the use of deicing salts and/or chemicals and mechanical removal. HPS, instead, uses concrete-embedded solutions to melt them.[119] However, the application of CF-based ECON in electrically heated pavements has emerged as a promising alternative. Using finite element analysis, the researchers of Reference 54 investigated the optimum CF dosage for HPS and concluded that ECON could effectively melt ice and snow on pavement surfaces.

Other research works by the authors[120] showed that the addition of a calcium nitrite-based corrosion inhibitor admixture as a conductivity-enhancing agent (CEA) improved the electrical conductivity and compressive strength of ECON, particularly for samples with low fiber content. This enhancement made the HPS more effective in melting ice and snow. In addition, a third work[121] studied the feasibility of using polyurethane-carbon-microfiber (PU-CMF) composite coating for heating pavement. It was found that the composite coating has great potential in the HPS application due to its durability, surface friction, and volume conductivity. However, the high construction cost was identified as a limitation.

3.5.4 | Corrosion monitoring

Interesting applications can be found for cement-based sensors as well. To provide one example, smart concrete solutions can be employed to monitor corrosion inside RC components, as reported by Reference 122. In this example, cement-based embedded piezoelectric sensors were used to monitor cracking and corrosion onset through acoustic emissions. The study involved using a 3% NaCl solution in plexiglass dams. These were placed at the center top of RC beams to induce corrosion caused by the chemical solution's ingress. The experimental setup, performed with corrosion only or coupled corrosion plus mechanical loading, is detailed in Figure 10.

The results indicated that piezoelectric composite sensors possess significant potential for damage monitoring, including corrosion, due to their good durability and high sensitivity.

In a similar experiment, Reference 123 demonstrated that CF sensors installed on the concrete surface are

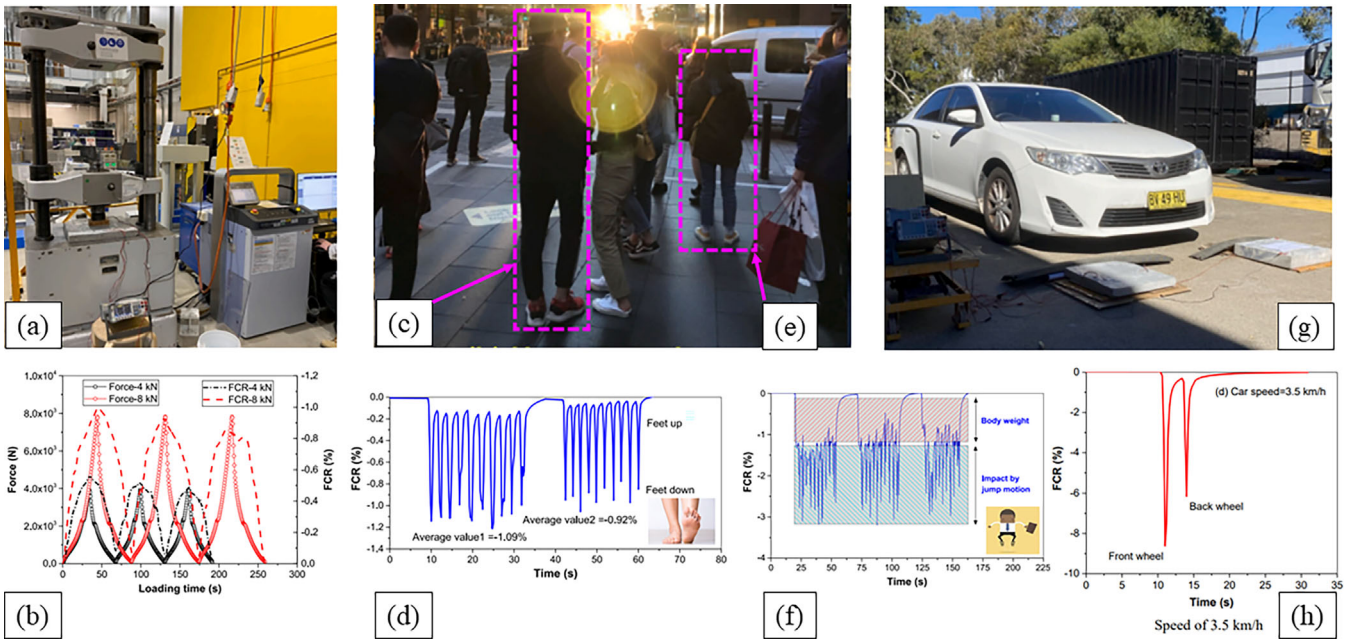

FIGURE 11 Smart mortar slabs with embedded cement-based sensors undergoing laboratory uniaxial compression test (setup (a) and results (b)), human motion simulations (feet up-feet down (c and d), and jump test (e and f)), and vehicle speed tests (as before, setup on the top row (g), and results on the bottom row (h), for the highest speed tested). Adapted from Reference 124.

effective for locating and assessing corrosion of steel reinforcements with high accuracy. Overall, the laboratory experiment concluded that embedded cement-based piezoelectric sensors are suitable for corrosion monitoring in concrete structures, highlighting the potential of self-sensing sensors for SHM.

4 | RECENT AND NOTEWORTHY FIELD APPLICATIONS OF SSC

Since SSC (especially ISSC) is a relatively new framework, many solutions remain in the research phase, with limited validation apart from small-scale samples in a controlled laboratory environment. To further stress the feasibility of the application of ISSC solutions in everyday practice, three examples of field-tested ISSC studies are reported here, chosen from the reviewed papers.

4.1 | Vehicle speed and human motion

The study reported in Reference 124 was intended as a proof of concept for transportation monitoring, in the sense of pedestrian motion detection and vehicle speed monitoring. According to the authors of Reference 124, the aim of their experimental investigation was to promote the practical applications of cement-based sensors in concrete pavement or roads, thereby achieving Smart Concrete infrastructures. From a SHM perspective, traffic load monitoring can be a noteworthy contribution to the fatigue assessment of existing infrastructures,[125] as also pointed out by the recent growing interest in weigh-in-motion technologies (see e.g.,[126–128]), which are nevertheless hampered by their high cost in their traditional format.

In this study, 1 wt.% CNF-based sensors were connected in series to form a 3 × 3 grid, embedded in small-scale (450 × 450 × 120 mm) mortar slabs.

The sample preparation involved dispersing CNF in a superplasticizer/water solution, mixing it with cement and silica fume to create an electrically conductive paste, casting specimens in molds with embedded electrodes, and curing them for 28 days.

For human and vechicle motion detection, several typologies of tests were performed, including laboratory tests (Figure 11a) and field tests. These latter ones included a Feet Up and Down Test (Figure 11c), a Jump Motion Test (Figure 11e), and a Vehicle Speed Detection test. For this last test, a 2013 Toyota Camry Altise was driven upon the Smart Mortar slabs (Figure 11g).

All tests returned good results. For cyclic compression tests, FCR variations followed well the loading and unloading phases, both at 4 and 8 kN, even if a performance decrease was observed peak after peak (see Figure 11b). This hysteretic effect was observed in many

other studies; this point will be further addressed in the following sections. In the case of the Feet Up and Down Test, the FCR values ranged from approximately −1.3% to −1.0% when the feet were fully on the slab to around −0.15% as the feet moved up (Figure 11d). The average value of FCR at the peaks was approximately −1.09%, corresponding to the first 10 cycles. However, it decreased to −0.92% in later cycles after preloading. For the Jump Motion Test, dynamic loads from jumping generated FCR peaks ranging from −2% to −3%. FCR changes out of static body weight (i.e., dead loads) were around 1%, resulting in the initial offset visible in Figure 11f. However, the FCR values did not come back to their initial value after jumping due to pushing force and hysteretic behavior. Finally, for the vehicle speed test, the sensors were capable of detecting the front and back wheels (Figure 11h). Furthermore, a strong correlation between the FCR and vehicle speed was found. In particular, FCR seems to logarithmically decrease with the vehicle's increasing speed (the tests, however, were all performed at very low velocities: 2.0, 2.2, 3.0, and 3.5 km/h), indicating that the sensor could measure and track vehicle velocity.

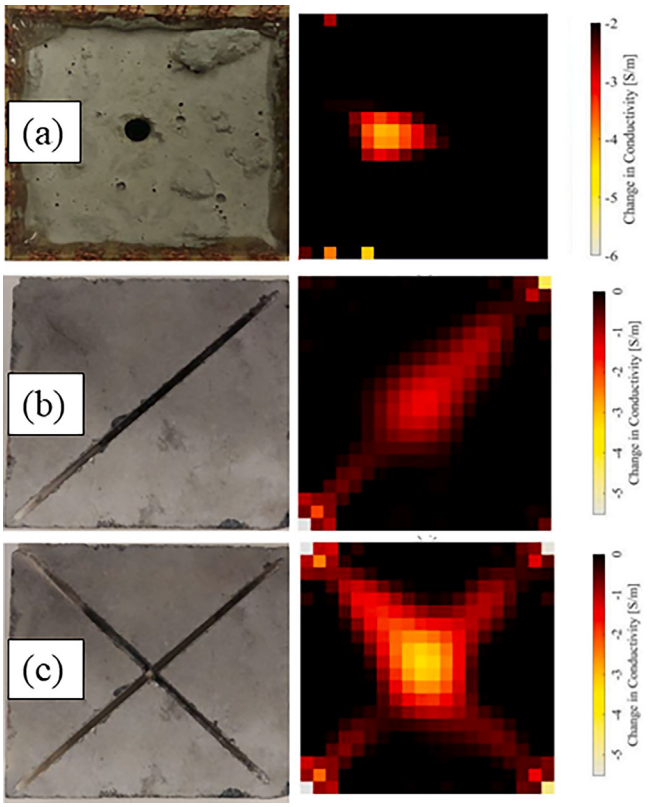

FIGURE 12 ERT results for (a) drilled hole, (b) single, and (c) double diagonal cuts. Retrieved from Reference 129. ERT, electrical resistance tomography.

4.2 | Traffic detection and monitoring pavement system

In 2021, in situ crack mapping of a large-scale concrete pavement was performed by Reference 129 to validate the field application of ISSC in airport pavements. Electrical resistance tomography (ERT) was utilized to map conductivity distributions and identify spatially distributed damage features.

Multi-walled CNT thin films were added to the cement–aggregate interface via spray coating.[104] Concrete casting was carried out directly using the MWCNT thin film-coated fine and coarse aggregates. To optimize ERT damage sensitivity and signal-to-noise ratio, prior research[130] was taken into consideration when designing the SSC mix.

Conceptually, conductivity maps were obtained by recording voltage readings to identify the positions, forms, and degrees of internal damage features, such as cracks and subsurface defects. Figure 12 shows a representation of single and multiple damage detection and localization using cuts made on samples. Specimens with different sizes (100 × 100 mm, 200 × 200 mm, and 300 × 300 mm) were tested, with different typologies and extensions of artificially added macroscopic damage. The results in the specimens showed that the insertion of progressive damage caused gradual conductivity changes. Extended holes with significant conductivity increases, as well as smaller drilled holes with moderate conductivity changes, could both be accurately identified.

For full-scale testing, a 15 × 12 ft (4.6 × 3.6 m) pavement concrete slab with four 18 × 12 in (0.46 × 0.30 m) Smart Concrete regions was cast. The SSC regions were cast using the same mix design as the rest of the pavement. The slab with embedded sensors (Figure 13a–e) was then subjected to Heavy Vehicle Simulator (HVS) testing to mimic the loading conditions experienced by airport pavements by applying aircraft wheel loads to the pavement. These simulated long-term effects of aircraft traffic caused cracks and other kinds of damage in the concrete pavement.

In this field application, the methodology correctly identified and mapped subsurface (non-visible) cracks and material flaws, as verified with ERT detection (see Figure 13f,g for an example). In real-life applications, this is expected to allow for early warning and timely maintenance scheduling in pavement management.

4.3 | Weigh-in-motion SSC

The research study reported in Reference 131 describes an application of self-sensing concrete with CNTs for

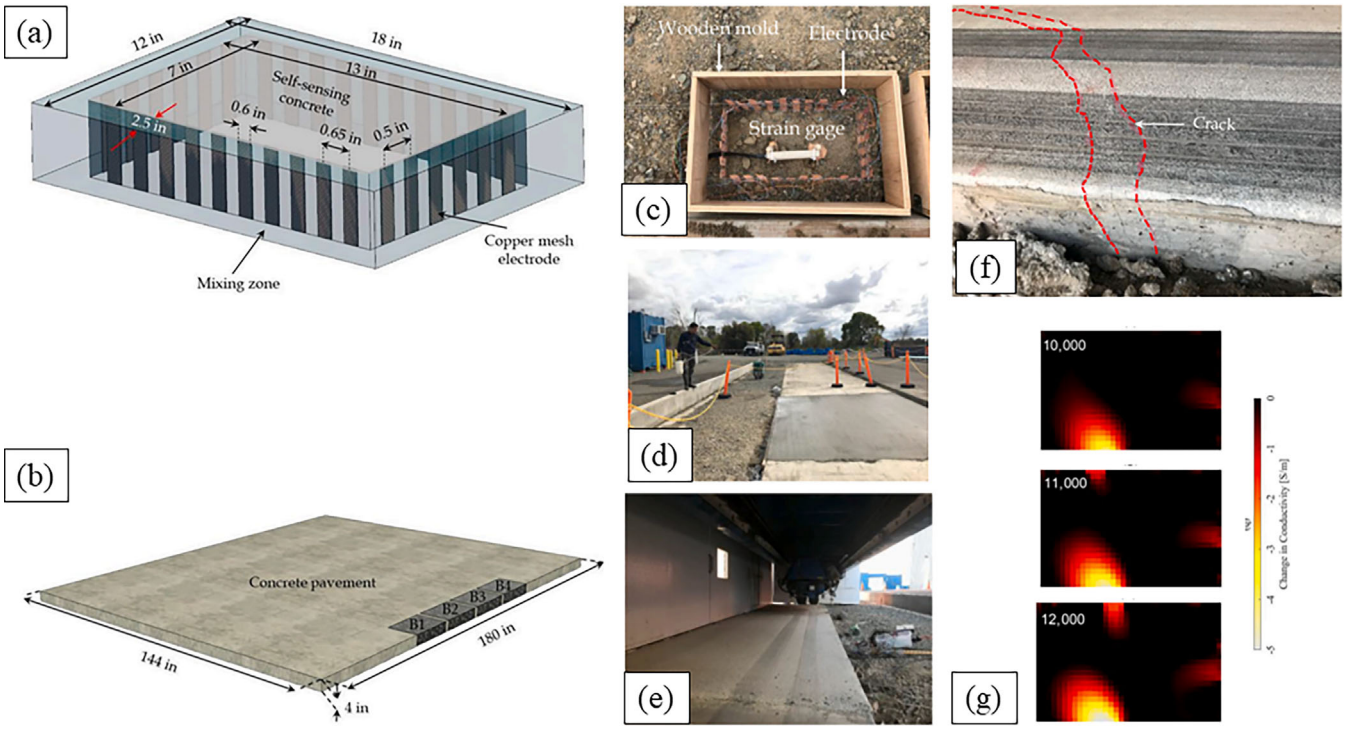

FIGURE 13 (a) Geometry and size (0.46 × 0.30 × 0.10 m) of the self-sensing concrete boxes cast as a part of the (b) 4.6 × 3.7 m full-length airport pavement slab, with the four smart concrete sections indicated with B1–B4. (c–e) Casting of self-sensing concrete boxes for the field test: before, immediately after, and after curing (28 days). (f and g) Crack initiation comparison with ERT results as 11,000 cycles showing successful crack detection. Adapted from Reference 129. ERT, electrical resistance tomography.

roadside vehicle detection. Pre-cast and cast-in-place self-sensing CNT concrete sensors (Figure 14a,b) were integrated into a controlled pavement test section at the Minnesota Road Study Facility (MnROAD), USA. Road tests were carried out under a variety of environmental situations with a five-axle semi-trailer tractor-truck and a relatively smaller van (Figure 14d,e). To compare the effectiveness of CNT concrete sensors against conventional strain gauges (installed in both the cast-in-place and pre-cast variants) for vehicle detection accuracy, the analysis concentrated on measuring the electrical resistance changes in the sensors in response to passing heavy and light vehicles (Figure 14f).

The strain gauge recordings were compared with the CNT concrete sensors' voltage signals, showing that both types of sensors detected the presence of a truck at the same time as it passed over them. Additionally, the CNT concrete sensors seemed to exhibit better detection accuracy than the strain gauges. The authors explain this result due to the greater sensing surface of the CNT sensors, which should enable more thorough data collecting. Finally, comparing the test results at different speeds and with different vehicles, it was indicated that the CNT concrete sensors consistently exhibit stable and repeatable capabilities for detecting traffic flow. Nevertheless, the authors highlighted that the limited sample size for road tests may impact the generalizability of results. Also, they pointed out many general issues of ISS that will also be discussed later in Section 5 in more detail: outdoor environmental factors such as weather conditions could influence sensor performance; maintenance requirements for CNT sensors may be higher compared to conventional (surface-attached) sensors; further research needed to explore the long-term durability and reliability of CNT sensors; and that the cost implications of implementing and upkeeping CNT concrete sensors on a larger scale need to be assessed.

5 | DISCUSSION AND KEY CONSIDERATIONS

From the reviewed scientific articles, a few points have emerged that should be attentively considered when designing an ISSC system. These are listed here below.

5.1 | Effects of setup parameters

The first key point is that, all else being equal, ISSC systems respond differently to different setups—namely, loading conditions and electrical parameters.

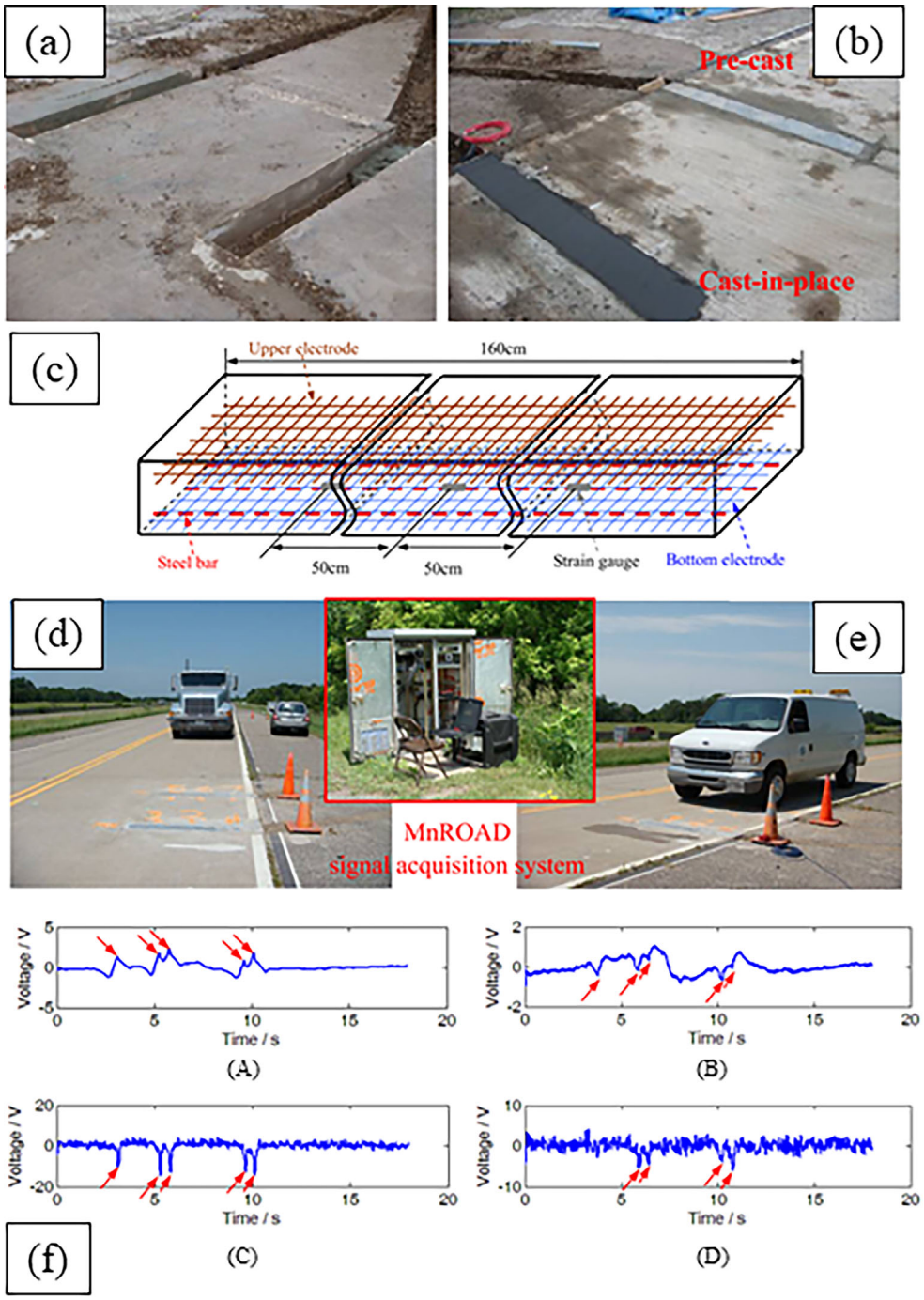

FIGURE 14 (a and b) Setup and casting of the self-sensing pavement tracts. (c) Self-sensing concrete setup with electrodes, steel bars, and strain gauges. (d and e) Road test setup with the five-axle semi-tractor trailer truck and the lighter van. (f) Results of truck passing at a higher speed of 20 mph (32 km/h): (A) cast-in-place CNT concrete sensor, (B) pre-cast CNT concrete sensor, (C) strain gauge in the middle of the cast-in-place CNT concrete sensor, and (D) strain gauge in the middle of the pre-cast CNT Adapted from Reference 131. CNT, carbon nanotube.

Regarding these latter ones, both the anode and the cathode must be connected to the composite, and the flow of current should be directed from the anode toward the cathode. The sensor should be connected to an LCR meter, which is an electronic device used for measuring inductance (L), capacitance (C), and resistance (R). The LCR meter can be used to measure the electrical conductivity, resistivity, and permittivity using electrical impedance spectroscopy (EIS). EIS applies an AC to the sensor and measures impedance rather than direct resistance. As discussed before, AC is preferred for cement-based sensors to reduce or minimize electrode polarization. The polarization of DC leads to changes in resistance over time as the sensor or capacitor becomes charged and thus can generate opposing currents.[132]

For all the reasons reported here and in previous Sections, the use of a four-probe setup is strongly encouraged over the relatively easier, yet less accurate, two-probe alternative. Electrode placement is particularly critical in flexural testing scenarios, such as three-point bending tests, where electrodes should ideally be positioned close to support regions.[133]

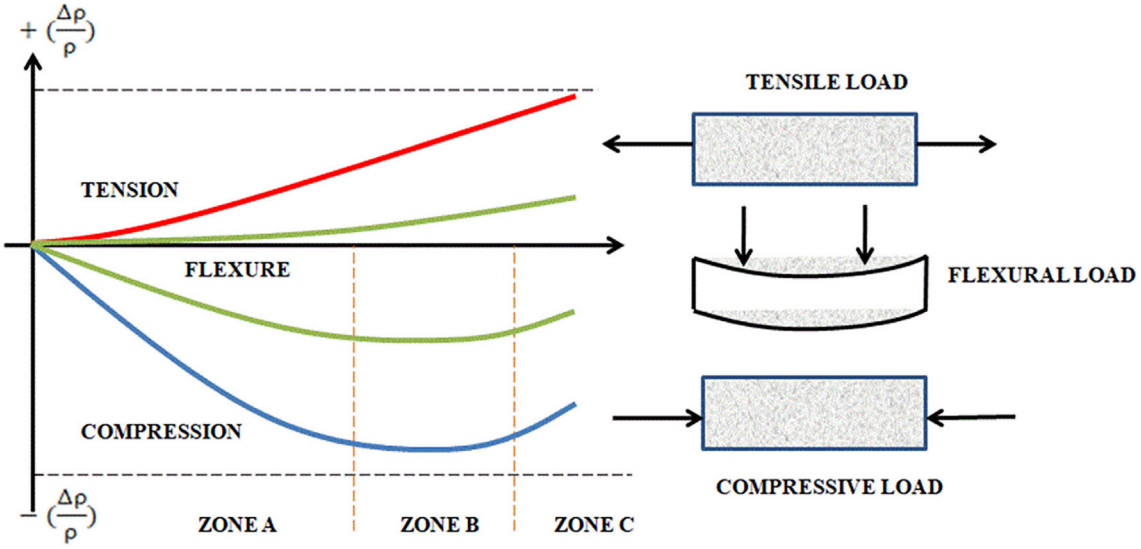

FIGURE 15 Graphical representation of FCR for different loading conditions. Image retrieved from Reference 32. FCR, fractional change in (longitudinal) electrical resistivity.

It is noted that EIS measurements occur across a specific frequency range. For cement-based sensors, a frequency range of 0.1–100 kHz is commonly used. Literature indicates that at 100 Hz, the impedance remains practically constant, indicating proximity to its real part. The upper limit serves as a reference value for electrical resistance.[133]

A few considerations are essential for real-life field applications regarding the different loading conditions. In fact, not all load scenarios can be detected by employing ISSCs—or detected with the same accuracy.

In general terms, samples of the Smart Concrete of interest should be preliminarily laboratory tested in a controlled environment for (i) pure tensile, (ii) pure compressive, and (iii) flexural (bending) conditions before in situ deployment. When performed with increasing quasi-static loads, these tests will determine the minimum critical load for detectability and the tolerance of the measurement. For damage detection purposes, they should preferably be carried on till failure, also tracking the occurrence and growth of visible (e.g., surface) cracks. Tests with dynamic loads can be performed as well to evaluate the Smart Concrete capabilities to identify sudden changes in FCR. In this case, multiple cycles of increasing and decreasing loads are typically applied. It is suggested that these cyclic test procedures should be applied for all load configurations.

As graphically shown in Figure 15 for the three loading conditions of interest, bending-induced strain states are the most difficult to accurately estimate. As already mentioned in the earlier Sections, this derives from FCR being directly proportional to the axial strain, which is not constant along the cross-section of a bent beam element. Conversely, pure compression/pure traction results in uniform shortening/elongation, which results in more clearly defined increases/decreases in FCR. In this regard, compressive strength is not monotonic due to concurring phenomena. In the first phase, under compaction pressure, the distance of conductive particles decreases, thereby improving the conductive network within concrete (zone A). Then, this is compensated by the destruction/reconstruction of the conductive network, in concomitance with the development of microscopic cracks (zone B). Finally, the expansion of cracks results in the disruption of the conductive network (zone C).[46]

If the resulting mechanical stresses did not exceed the elastic range of the composite, upon unloading, the FCR should return to its initial value, reflecting the elastic recovery of the material.[67] The potential occurrence of cracks not recovered during unloading would result in a residual FCR value due to the newly added contact resistivity. These irreversible changes in the electrical resistance of the composite are a strong damage-sensitive feature for the embedded structure[65]; however, fiber and nanotube damages, unrelated to the macroscopic health condition of the composite as a whole, may cause resistivity drops as well in the long term. The issue of these confounding influences has not yet been completely solved.

5.2 | Effects of different fillers on sensitivity parameters

Table 6 summarizes the effects of different functional fillers at different volume fractions on three sensitivity

TABLE 6 Some examples of sensitivity comparison of different fillers.

Filler type	Mix type	Percentage of filler (vol.%)	Sensitivity parameters			References
			FCR (−)	Gauge factor (−)	Resistivity (Ωm)	
SF	Cement mix	0.50	–	350.82 before cracking, 87.26 after	1.35×10^3	12
		1.00	–	364.35 before cracking, 155.98 after	1.05×10^3	
		1.50	–	374.34 before cracking, 164.44 after	1.05×10^3	
		2.00	–	417.62 before cracking, 156.44 after	0.91×10^3	
	Cement mortar	1.50 (30 mm long twisted SFs)	–	138.09	0.55×10^3	143
		1.50 (30 mm long smooth SFs)	–	99.85	1.09×10^3	
		1.50 (30 mm long hooked SFs)	–	88.50	1.75×10^3	
		1.50 (20 mm long twisted SFs)	–	139.68	1.14×10^3	
		1.50 (19 mm long smooth SFs)	–	99.70	3.52×10^3	
		1.50 (13 mm long smooth SFs)	–	52.90	6.29×10^3	
	Concrete	1.00 (30 mm long smooth) + 1.00 (19 mm long smooth), Type 0.8 cement	0.73	–	0.21×10^3	144
		1.00 (30 mm long smooth) + 1.00 (19 mm long smooth), Type 1 cement	0.45	–	0.97×10^3	
CF	Cement paste	0.5	0.72	160.3	–	145
	Concrete	0.50 (5 mm long CF)	0.37	–	–	125
		2.00 (5 mm long CF)	1.01	–	–	
		3.00 (5 mm long CF)	1.32	–	–	
Nano GP	Cement paste	5.00	–	156.00	–	146
CF, CNT	Cement paste	0.10 CF, 0.50 CNT	0.25	160.30	–	145
		0.15 CF, 0.01 CNT	0.23	–	–	67
SF, CNT	Concrete	2.00 straight 13 mm long SF, 0.50 CNT	0.24	67.80	–	139
		2.00 straight 19.5 mm long SF, 0.50 CNT	0.33	46.40	–	
		2.00 straight 30 mm long SF, 0.50 CNT	0.63	36.50	–	
		2.00 twisted 30 mm long SF, 0.50 CNT	0.59	39.00	–	
Conductive clay, CF	Mortar	50.00 clay, 0.60 CF	0.13	–	–	125
		30.00 clay, 0.60 CF	0.17	–	–	
		30.00 clay, 0.90 CF	0.16	–	–	

Abbreviations: CF, carbon fiber; CNT, carbon nanotube; FCR, fractional change in (longitudinal) electrical resistivity; GP, graphite powder; SF, steel fiber.

parameters: the aforementioned FCR, base material piezoresistivity ρ_0, and the GF. Regarding this last parameter, it should be recalled that higher values are preferable since they amplify the strain estimated from the very low sensed FCRs. For other examples of similar studies, refer to References 112,134–142.

5.3 | Effects of different fillers on macroscopic mechanical properties

As mentioned, the addition of conductive filler often involves a decrease in the mechanical properties of the Smart Concrete with respect to its original counterpart;

this applies either to conventional RC[147] and UHPCs.[148] The root cause is generally the disruption of the concrete matrix induced by the presence of the conductive network. The scientific literature contains numerous studies related to the effect of CFs and SFs on the compressive and flexural strength of the composite mix, whereas only with more recent developments there have been studies regarding CNTs and other nano-based fillers.

Regarding the ultimate compressive strength of the material, the incorporation of different percentages of CNTs and nanofibers may have different effects on the relative compressive strength of the composite mix. In general terms, the compressive strength may increase with the increase in the filler content but decreases beyond a critical value.[149–152]

According to Reference 149, when carbon nanofillers are widely dispersed, they can embed or coat within hydration components, such as the amorphous C–S–H gel. This process serves to reinforce the hydrates by acting as inert fillers for gel pores and creating bridges between adjacent gel particles. Also, it promotes the formation of denser C–S–H gel, enhancing stiffness and resisting crack formation and propagation through pinning, bridging, and pull-out effects, thus absorbing loading energy.

On the contrary, during the mixing process, nano-additives possess a high specific surface area and strong water absorption capacity, which leads to the absorption of free water and superplasticizers. This absorption increases the plastic viscosity of the fresh paste, hindering the escape of entrapped air. Also, the formation of flocculating constituents can hinder the hydration process by separating clinker and water. An increased dosage can result in the emergence of two weak zones within the matrix, that is, harmful pores (large capillary pores and air holes with pore size exceeding 50 μm) and agglomerated nanofiller bundles.[149,150]

The effect on mechanical properties by zero-dimensional carbon nanofillers (CNB) is more accentuated, possibly due to their sphericity, which causes a lack of cohesion and frictional resistance within the cement-based matrix. Also, nanoscale CNB, characterized by high surface energy, may capture cement particles and trap water, influencing cement hydration and hardening processes. Thus, they exhibit negative effects on mechanical properties comparable to one-dimensional (e.g., CNT, TWCNT, CNF) and two-dimensional (e.g., GNP) carbon nanofillers. These effects compete and reach equilibrium at the coefficient of inconsistency (CIC) with changes in the amount of carbon nanofillers incorporated. It is also observed that the compressive strength of ISSC decreases monotonically with increasing CNB content, indicating the positive effect on mechanical properties brought by zero-dimensional CNB.[51] Conversely, some studies (e.g., Reference 153) propose the use of some of these functional fillers, such as high volumes of fly ash, to improve some mechanical properties (e.g., tensile ductility) even if at the cost of reduced ultimate compressive and tensile strength, and/or to design strain-hardening cementitious composites.

Regarding the flexural strength of Smart Concrete for nanotubes, nanofibers, and SFs, the cohesive bond between the fibers and the matrix enhances the crack resistance of the flexural behavior, due to the bridging effect of the fibers.[149] On the other hand, functional fillers can also interfere with the cement matrix causing negative effects which lead to multiple visible cracks in regions where the matrix is weaker than the bond.[141,150,151] Some studies have reported inconsistent results[56]; nevertheless, many cases present strengths much larger than 100%, even up to 225%. However, as for UHPCs, it should be recalled that increased ultimate strength could be achieved at the cost of ductility and other key factors.[56,150,151]

The lower elastic limit in comparison to plain concrete is, as for the ultimate strength, generally attributed to the disruption of the concrete matrix, which causes a loss of elastic deformation capacity.

6 | CURRENT CHALLENGES AND FUTURE DIRECTIONS

In this Section, the limitations and challenges associated with the applicability of ISSC are discussed; potential solutions are proposed as well.

6.1 | Durability and longevity

The main difficulties for ISSC's survivability over an extended period arise from environmental exposure and material compatibility. The potentially damaging factors include temperature, moisture content, and humidity. In particular, moisture in concrete can change the conductivity of concrete composite mix. In wet or cold regions, factors such as the dry-wet cycle, ice formation, and the freeze–thaw cycle can negatively influence the electrical resistance of self-sensitive concrete over time. All these degradation effects result in the reduction of the lifetime and accuracy of the sensing capabilities of the cement composite.

Unlike physically attached sensors, embedded sensing capabilities cannot be replaced following sensor faults. Furthermore, the structural components (where the functional fillers are mixed in) need to last as long as the

project's required design life, which can be in the order of 50 or 100 years for critical RC infrastructures. Even common RC is well-known for its degradation issues during such long timeframes.

Material compatibility is another important factor when dealing with the durability of self-sensing systems. As ISSC involves the incorporation of different materials in the concrete mix, these materials need to be compatible with each other for accurate results in the sensing mechanism. Potential incompatibilities which produce negative results may occur due to differences in thermal expansion coefficients, unwanted chemical reactions, or different mechanical properties between the incorporated materials and concrete mix.[154] For example, when using nanomaterials within the composite mix, specific dispersing agents and techniques are necessary for accurate sensing results. Thus, this compatibility between the materials to be incorporated and the concrete mix greatly influences the durability and reliability of ISSC.

6.1.1 | Potential solutions

Several alternatives can be investigated, independently or jointly. For instance, protective coatings, encapsulation techniques, and/or improved fillers should be studied. It is also possible to optimize the sensor-concrete interface and compatibility, for example, by employing novel surfactant compositions during the mixing phase. Dispersion techniques, especially for what concerns nano-based composites, should be refined by means of laboratory tests. Finally, self-sensing can be paired with self-healing[155] capabilities. However, incorporating both technologies at once will increase complexities and measuring parameters, decreasing reliability.

6.2 | Limited sensing range and accuracy

The sensing range refers to the distance over which any sensor can effectively detect and measure the desired physical properties. In ISSCs, the "sensors" are embedded within the concrete matrix, which inherently expands the range to wherever the enhanced cement is cast but limits their ability to sense properties beyond a certain distance from their location in other structural components. In this regard, signal attenuation is an issue. As the electrical signals travel through the conductive network inside the concrete matrix, they experience attenuation, meaning they gradually weaken with distance. This attenuation reduces the effectiveness over greater distances. The properties of the concrete itself, such as its composition, density, and moisture content, can affect the propagation of sensing signals. Finally, external factors such as electromagnetic interference or physical obstructions within the concrete can interfere with the sensing range.

Furthermore, the accuracy of the sensors in SSC may vary depending on the same factors, that is, signal interferences and environmental conditions, plus due to improper sensor calibration. This results in lesser accuracy in the data with a significant limit on the effectiveness of the SHM system. Previous studies have shown that temperature and humidity can alter or interfere with accurate sensing mechanisms.[154,156] Of course, the quality of the dispersion in the mixture plays a major role as well.[157]

6.2.1 | Potential solutions

Regarding the sensing range, affordable and cost-effective sensor designs and manufacturing techniques will help. Regarding sensor accuracy, solutions at the hardware level are difficult to foresee, at least in the current framework. Thus, it is most likely that future advancements in these regards will be carried by software developments. For instance, novel and more effective algorithms and calibration techniques could increase the sensing accuracy.

6.3 | Confounding influences of shrinkage and creep

Concrete shrinkage (i.e., the volumetric decrease induced by a change in the moisture content) and creep (increased strain and deformation under equal but sustained loading over time) are two potential confounding factors. As damage-unrelated deformations, they affect the viability of strain monitoring as a damage proxy. In particular, the effects of shrinkage may be quite relevant. Nominally identical specimens with CF, CNT, and CB have been proven to perform differently after 7, 28, 90, and 180 days of curing.[158] Variations induced by the moisture content have been reviewed in detail in Reference 159.

Conversely, in a damage-free scenario (e.g., during concrete curing), ISSC may be used to monitor concrete drying, due to their humidity-sensitive property. This mainly happens due to water absorption/desorption at the filler–matrix interface; basically, the presence of water affects the contact resistance between the filler and the matrix, thus leading to variation in the bulk electrical resistance of sensing concrete.[46]

6.3.1 | Potential solutions

The admixture of short fibers itself has been proven to decrease drying shrinkage (see e.g. Reference 160). To further reduce unwanted concrete shrinkage, Reference 161 investigated the effects of added expansive agents and shrinkage-reducing admixtures on the self-sensing properties of CB-enhanced mortars.

6.4 | Periodic calibration and maintenance

As for any sensing device, improper calibrations can result in erroneous or inaccurate measurements and below-average SHM performance of the sensor. In ISSC materials, calibration is a complicated issue, both at the beginning and at periodic times for recalibration. This issue is exacerbated by the aforementioned low durability of many fillers, as well as by the need for high precision and reliable measurement to detect damage growth in its earliest stages. This contrasts with the relatively low repeatability of measurement even in newly-casted, non-aged specimens, even without accounting for the effects of prolonged outdoor exposure to harsh environmental conditions. For all these reasons, the calibration of Smart Concrete solutions currently requires skilled operators and careful implementation. This hampers their widespread use and raises the related costs.

Also, since damaged sensing capabilities cannot be repristinated (differently from removable surface-attached sensors), the recalibration issue is critical. Thus, engineers and SHM system designers need to develop a strict schedule for regular upkeep and long-term performance optimization.

6.4.1 | Potential solutions

It is suggested to utilize specialized and standardized equipment and expertise for accurate calibration at the deployment in situ and to establish a recalibration schedule, either time-fixed or condition-based, according to the expected durability of the filler and the other components of the concrete mix.

6.5 | Cost and scalability

The implementation of ISSC can be costly due to both initial installation and subsequent maintenance.

The initial costs are currently high or very high due to the expensive nano- and micro-materials to be incorporated into the concrete matrix. This can significantly impact the overall price of the building project. However, effective techniques such as nano-engineering the aggregates could greatly reduce the associated cost, thus allowing successful implementation of SSC at the industrial level, also profiting from scale economy if and when their use becomes more mainstream.

The lower workability of ISSC compared to conventional RC also increases construction costs, as attested for CF, CNT, and others,[162] with different levels of severity. All these functional fillers require the further use of superplasticizers or high-range water reducers to compensate, making them costlier.

Long-term maintenance costs are another major drawback due to the current low durability and the nature of a material-embedded solution. As mentioned, unlike physically attached sensors, the conductive components inside the concrete cannot be removed and replaced unless a very complicated and expensive retrofitting or partial reconstruction work is performed.

In this regard, low-cost materials, fabrication techniques, and pouring techniques will be needed for large-scale applications in everyday construction sites.

The industrial development of Smart Concrete is further potentially hampered by legislative issues, which will require the development of standards, codes, and protocols, as well as the scalability issues of the SHM framework as a whole; that is to say, the massive collection, processing, and analysis of big data generated by ISSC systems, which is a yet unsolved challenge on its own.

6.5.1 | Potential solutions

Novel budget-friendly materials (fly ash, silica fume, etc.), mixture designs, and (if possible, automated) manufacturing processes, such as the very recently proposed use of 3D printed self-sensing cementitious composites[163], can be explored and tested. Also, artificial intelligence can be used to optimize the fabrication process of the SSC, resulting in lower costs.[164]

6.6 | Data processing and interpretation

The main difficulties in the ISSC data analysis process stem from the large amount of data to be processed and the need to perform it as much as possible in an unsupervised fashion. These are the same main requirements as for any permanent, extensive SHM system, with the added difficulty of the (often) low repeatability of the measurements and the difficult interpretation of the

data[154,156] Another issue rarely addressed in the current literature is that the conductive ISSC materials exhibit dielectric properties that result in the accumulation of charge when subjected to a constant electric field. This accumulation generates an electric field that opposes the applied field. As a macroscopic effect, this behavior leads to a decrease in the electric current flowing through the material over time when a constant voltage is applied.[165]

Furthermore, as for any SHM system, sensed raw data needs to be converted into usable information; however, these are software-related aspects that deviate excessively from the aims of this review.

6.6.1 | Potential solutions

Data processing and intepretation will need the development of computationally efficient, robust, and scalable software solutions, that is, algorithms and data analysis techniques, potentially also fast enough to enable real- or quasi-real-time signal processing and analysis. In particular, big data analysis can benefit from the latest advancements in machine learning (ML) and artificial intelligence to automate the interpretation of the sensor data.[166] ML algorithms can be used to train systems based on experimental data to detect damages or cracks within the self-sensing systems.[167,168] Artificial neural networks (ANNs) can be used to predict concrete properties such as compressive strength as well as electrical resistivity.[169] The research work described in Reference 170 reports a comparison between traditional techniques and Deep ANNs for damage detection and localization via EIT, testing both MWCNT and graphene nanosheets (GNs). Finally, apart from data interpretation, user-friendly software tools with intuitive graphical user interfaces and visualization will be needed to expand the accessibility and easiness of use to non-expert operators.

6.7 | Concluding remarks on current limitations for industrial uses

In 2019, the authors of Reference 171 presented the results of an interesting survey of 78 experts, including consultants and clients from the concrete industry sector. The responses highlighted the following points as the main limitations to the widespread use of ISSC: upfront costs of the material (61.5% of the respondents), lack of industry standards and guidance (ca. 50%), technical understanding (35.9%), and lack of familiarity (slightly less than 35%).

As already discussed in the previous parts of this dedicated Section, most of these aspects remain to be solved five years later. However, from a comparison with a similar previous survey (2017) from the same first author[172], the respondents' familiarity with ISSC increased from 32% to 37%; hence, it is likely that the public perception of these innovative sensing solutions has been improving since then.

7 | CONCLUSIONS

In Italy, Western Europe, and most of the developed countries, the aging of concrete structures and infrastructures poses a relevant structural risk. SHM and novel construction materials are both needed to ensure a safer and more resilient built environment. By integrating load-bearing and sensing capabilities, Smart Concrete is intended to address all these necessities.

This review work was primarily aimed at assessing the applicability of resistance-based ISSC solutions for uses in civil engineering. Based on reported experimental tests with both laboratory and field validations, these novel technologies are justified not only for SHM but also for traffic detection, temperature and hydration monitoring, and other related applications. For SHM purposes, all these recorded data can provide important insight both on damage development—for example, crack initiation and growth, as well as degradation-induced loss of material strength—and damage-unrelated ambient effects.

The limitations and challenges posed by these technologies have been thoroughly discussed, coupled with the solutions proposed by several authors in the published scientific literature to date. Arguably, there is still room for technical improvement. The large-scale implementation of ISSC in standard construction practices will require these advancements.

Based on the findings of this review work, it is advised to use Smart Concrete solutions only after proper laboratory calibration with destructive tests, performed over a statistically relevant number of specimens and using different setups and loading conditions. For field application, the use of ISSC in structural subcomponents under constant compressive or tensile stress, such as bridge piers, should be preferred over their use in components mainly undergoing bending stresses such as bridge decks. Under long-term cyclic loads, such as the ones induced by seasonal or daily temperature fluctuations, residual changes in resistivity can be linked to the occurrence of cracks inside the material, thus allowing for damage detection and diagnosis. The use of diffuse ISSC throughout several components or at different positions would also potentially allow for damage localization. However, these potential applications are hampered by the relatively low durability of the current functional fillers over prolonged use.

Nevertheless, the economic and practical potential of fully embedded, diffused self-sensing capabilities represents a compelling scenario for the construction industry. For these reasons, the current obstacles to their widespread use —such as limited sensing range, poor durability, need for periodic recalibration, high deployment and maintenance costs, and low scalability—will likely be overcome in the near future. These novel and promising hardware tools will pair well with the most recent advances in machine learning and artificial intelligence for damage detection and assessment.

ACKNOWLEDGMENTS

This work is part of the research activity developed by the authors within the framework of the "PNRR": MOST—Sustainable Mobility National Research Center—SPOKE 7 "CCAM, Connected Networks and Smart Infrastructure"—WP4 and received funding from the European Union NextGenerationEU (Piano Nazionale di Ripresa e Resilienza (PNRR) – Missione 4 Componente 2, Investimento 1.4 – D.D. 1033 17/06/2022). Open access publishing facilitated by Politecnico di Torino, as part of the Wiley - CRUI-CARE agreement.

DATA AVAILABILITY STATEMENT

Data sharing not applicable to this article as no datasets were generated or analysed during the current study.

ORCID

Marco Civera https://orcid.org/0000-0003-0414-7440

REFERENCES

1. Srinivasan AV, McFarland MD. Smart structures: analysis and design. Cambridge: University of Cambridge; 2001.
2. Chopra I. Review of state of art of smart structures and integrated systems. AIAA J. 2012;40(11):2145–87. https://doi.org/10.2514/21561
3. Gulisano F, Jimenez-Bermejo D, Castano-Solís S, Sánchez Diez LA, Gallego J. Development of self-sensing asphalt pavements: review and perspectives. Sensors. 2024;24(3):792 Available from: https://www.mdpi.com/1424-8220/24/3/792/htm
4. Xin X, Liang M, Yao Z, Su L, Zhang J, Li P, et al. Self-sensing behavior and mechanical properties of carbon nanotubes/epoxy resin composite for asphalt pavement strain monitoring. Constr Build Mater. 2020;10(257):119404.
5. Hasni H, Alavi AH, Chatti K, Lajnef N. A self-powered surface sensing approach for detection of bottom-up cracking in asphalt concrete pavements: theoretical/numerical modeling. Constr Build Mater. 2017;144:728–46.
6. Downey A, D'Alessandro A, Laflamme S, Ubertini F. Smart bricks for strain sensing and crack detection in masonry structures. Smart Mater Struct. 2017;27(1):015009 Available from: https://iopscience.iop.org/article/10.1088/1361-665X/aa98c2
7. Meoni A, D'Alessandro A, Cavalagli N, Gioffré M, Ubertini F. Shaking table tests on a masonry building monitored using smart bricks: damage detection and localization. Earthq Eng Struct Dyn. 2019;48(8):910–28. Available from: https://onlinelibrary.wiley.com/doi/full/10.1002/eqe.3166
8. Borke Birgin H, D'Alessandro A, Favaro M, Sangiorgi C, Laflamme S, Ubertini F. Field investigation of novel self-sensing asphalt pavement for weigh-in-motion sensing. Smart Mater Struct. 2022;31(8):085004 Available from: https://iopscience.iop.org/article/10.1088/1361-665X/ac7922
9. García-Macías E, Ubertini F. Earthquake-induced damage detection and localization in masonry structures using smart bricks and kriging strain reconstruction: a numerical study. Earthq Eng Struct Dyn. 2019;48(5):548–69. Available from: https://onlinelibrary.wiley.com/doi/full/10.1002/eqe.3148
10. Meoni A, D'Alessandro A, Kruse R, De Lorenzis L, Ubertini F. Strain field reconstruction and damage identification in masonry walls under in-plane loading using dense sensor networks of smart bricks: experiments and simulations. Eng Struct. 2021;15(239):112199.
11. Chopra I, Sirohi J. Smart structures theory. Cambridge: University of Cambridge; 2013.
12. Nguyen DL, Ngoc-Tra Lam M, Kim DJ, Song J. Direct tensile self-sensing and fracture energy of steel-fiber-reinforced concretes. Compos Part B Eng. 2020;15(183):107714.
13. Yoo DY, Kim S, Lee SH. Self-sensing capability of ultra-high-performance concrete containing steel fibers and carbon nanotubes under tension. Sens Actuators A Phys. 2018;276:125–36.
14. Sangoju B, Gopal R, Bhajantri HB. A review on performance-based specifications toward concrete durability. Struct Concr. 2021;22(5):2526–38. Available from: https://onlinelibrary.wiley.com/doi/full/10.1002/suco.201900542
15. Vereecken E, Botte W, Lombaert G, Caspeele R. Assessment of corroded prestressed and posttensioned concrete structures: a review. Struct Concr. 2021;22(5):2556–80. Available from: https://onlinelibrary.wiley.com/doi/full/10.1002/suco.202100050
16. Lu Y, Zhang J, Li Z, Dong B. Corrosion monitoring of reinforced concrete beam using embedded cement-based piezoelectric sensor. Mag Concr Res. 2013;65(21):1265–76.
17. Farrar CR, Worden K. Structural health monitoring: a machine learning perspective. Hoboken, New Jersey: John Wiley & Sons L; 2013.
18. Aloisio A, Di Battista L, Alaggio R, Fragiacomo M. Sensitivity analysis of subspace-based damage indicators under changes in ambient excitation covariance, severity and location of damage. Eng Struct. 2020;208:110235.
19. Alaggio R, Aloisio A, Antonacci E, Cirella R. Two-years static and dynamic monitoring of the Santa Maria di Collemaggio basilica. Constr Build Mater. 2021;268:121069.
20. Sun M, Staszewski WJ, Swamy RN. Smart sensing technologies for structural health monitoring of civil engineering structures. Adv Civ Eng. 2010;2010:1–13.
21. O'Shea M, Murphy J. Design of a BIM integrated structural health monitoring system for a historic offshore lighthouse. Buildings. 2020;10(7):131.
22. Reddy PN, Kavyateja BV, Jindal BB. Structural health monitoring methods, dispersion of fibers, micro and macro structural properties, sensing, and mechanical properties of

self-sensing concrete—a review. Struct Concr. 2021;22(2): 793–805. Available from: https://onlinelibrary.wiley.com/doi/full/10.1002/suco.202000337

23. Han B, Ding S, Yu X. Intrinsic self-sensing concrete and structures: a review. Measurement. 2015;59:110–28.
24. Cleven S, Raupach M, Matschei T. Electrical resistivity measurements to determine the steel fiber content of concrete. Struct Concr. 2022;23(3):1704–17.
25. Murray CM, Doshi SM, Sung DH, Thostenson ET. Hierarchical composites with electrophoretically deposited carbon nanotubes for in situ sensing of deformation and damage. Nanomaterials. 2020;10(7):1262.
26. Cassese P, Rainieri C, Occhiuzzi A. Applications of cement-based smart composites to civil structural health monitoring: a review. Appl Sci. 2021;11(18):8530.
27. Han B, Zhang L, Ou J. Smart and multifunctional concrete toward sustainable infrastructures. Singapore: Springer; 2017.
28. Li Z, Leung C, Xi Y. Structural renovation in concrete. Milton Park, Abingdon: Taylor & Francis Ltd; 2009. p. 1–348 Available from: https://www.taylorfrancis.com/books/mono/10.1201/9781482265972/structural-renovation-concrete-zongjin-li-christopher-leung-yunping-xi
29. Azarsa P, Gupta R. Electrical resistivity of concrete for durability evaluation: a review. Adv Mater Sci Eng. 2017;2017(1): 8453095 Available from: https://onlinelibrary.wiley.com/doi/full/10.1155/2017/8453095
30. Whittington HW, McCarter J, Forde MC. The conduction of electricity through concrete. Mag Concr Res. 2015;33(114):48–60. https://doi.org/10.1680/macr19813311448
31. Chung DDL. Self-sensing concrete: from resistance-based sensing to capacitance-based sensing. Int J Smart Nano Mater. 2021;12(1):1–19. Available from: https://www.tandfonline.com/doi/abs/10.1080/19475411.2020.1843560
32. Ramachandran K, Vijayan P, Murali G, Vatin NI. A review on principles, theories and materials for self sensing concrete for structural applications. Materials. 2022;15(11):3831.
33. Wang X, Ding S, Ni YQ, Zhang L, Dong S, Han B. Intrinsic self-sensing concrete to energize infrastructure intelligence and resilience: a review. J Infrastruct Intell Resilience. 2024; 3(2):100094.
34. Li W, Dong W, Castel A, Sheng D. Self-sensing cement-based sensors for structural health monitoring toward smart infrastructure. J Proc R Soc NSW. 2021;154:24–32.
35. Han B, Wang Y, Dong S, Zhang L, Ding S, Yu X, et al. Smart concretes and structures: a review. J Intell Mater Syst Struct. 2015;26(11):1303–45. https://doi.org/10.1177/1045389X15586452
36. Wen S, Chung DDL. Effect of stress on the electric polarization in cement. Cem Concr Res. 2001;31(2):291–5.
37. Kanagasundaram K, Solaiyan E. Smart cement-sensor composite: the evolution of nanomaterial in developing sensor for structural integrity. Struct Concr. 2023;24(5):6297–337. Available from: https://onlinelibrary.wiley.com/doi/full/10.1002/suco.202201145
38. Baoguo H, Yu X, Jinping O. Self-sensing concrete in smart structures. Oxford: Butterworth-Heinemann; 2015.
39. Cao J, Chung DDL. Improving the dispersion of steel fibers in cement mortar by the addition of silane. Cem Concr Res. 2001;31(2):309–11.
40. Chung DDL. Cement reinforced with short carbon fibers: a multifunctional material. Compos Part B Eng. 2000;31(6–7): 511–26.
41. Lee SJ, You I, Zi G, Yoo DY. Experimental investigation of the piezoresistive properties of cement composites with hybrid carbon fibers and nanotubes. Sensors. 2017;17(11):2516 Available from: https://www.mdpi.com/1424-8220/17/11/2516/htm
42. García-Macías E, D'Alessandro A, Castro-Triguero R, Pérez-Mira D, Ubertini F. Micromechanics modeling of the uniaxial strain-sensing property of carbon nanotube cement-matrix composites for SHM applications. Compos Struct. 2017;163: 195–215.
43. Hiremath N, Bhat G. High-performance carbon nanofibers and nanotubes. Structure and properties of high-performance fibers. Cambridge: Woodhead Publishing; 2017. p. 79–109.
44. Tian Z, Li S, Li Y. Enhanced sensing performance of cement-based composites achieved via magnetically aligned nickel particle network. Compos Commun. 2022;29:101006.
45. Tian Z, Li Y, Li S, Vute S, Ji J. Influence of particle morphology and concentration on the piezoresistivity of cement-based sensors with magneto-aligned nickel fillers. Measurement. 2022;187:110194.
46. Ding S, Dong S, Ashour A, Han B. Development of sensing concrete: principles, properties and its applications. J Appl Phys. 2019;126(24):241101 Available from: https://pubs.aip.org/aip/jap/article/126/24/241101/156653/Development-of-sensing-concrete-Principles
47. Rovnaník P, Kusák I, Bayer P, Schmid P, Fiala L. Electrical and self-sensing properties of alkali-activated slag composite with graphite filler. Materials. 2019;12(10):1616 Available from: https://www.mdpi.com/1996-1944/12/10/1616/htm
48. Dinesh A, Saravanakumar P, Rahul Prasad B, Kilbert Raj S. Carbon black based self-sensing cement composite for structural health monitoring – a review on strength and conductive characteristics. Mater Today Proc. 2023; in press. doi:10.1016/j.matpr.2023.03.661
49. Luo J, Zhang C, Li L, Wang B, Li Q, Chung KL, et al. Intrinsic sensing properties of chrysotile fiber reinforced piezoelectric cement-based composites. Sensors. 2018;18(9):2999 Available from: https://www.mdpi.com/1424-8220/18/9/2999/htm
50. Huang Y, Li H, Qian S. Self-sensing properties of engineered cementitious composites. Constr Build Mater. 2018;174: 253–62.
51. Tian Z, Li Y, Zheng J, Wang S. A state-of-the-art on self-sensing concrete: materials, fabrication and properties. Compos Part B Eng. 2019;177:107437.
52. Choi HJ, Kim MS, Ahn D, Yeo SY, Lee S. Electrical percolation threshold of carbon black in a polymer matrix and its application to antistatic fibre. Sci Rep. 2019;9(1):1–12. Available from: https://www.nature.com/articles/s41598-019-42495-1
53. Jinping O, Han B. Piezoresistive cement-based strain sensors and self-sensing concrete components. J Intell Mater Syst Struct. 2009;20(3):329–36.
54. Sassani A, Arabzadeh A, Ceylan H, Kim S, Sadati SMS, Gopalakrishnan K, et al. Carbon fiber-based electrically conductive concrete for salt-free deicing of pavements. J Clean Prod. 2018;203:799–809.

55. Dinesh A, Suji D, Pichumani M. Electro-mechanical investigations of steel fiber reinforced self-sensing cement composite and their implications for real-time structural health monitoring. J Build Eng. 2022;51:104343.
56. Wang H, Shi F, Shen J, Zhang A, Zhang L, Huang H, et al. Research on the self-sensing and mechanical properties of aligned stainless steel fiber-reinforced reactive powder concrete. Cem Concr Compos. 2021;119:104001.
57. Silvestro L, Gleize PJP. Effect of carbon nanotubes on compressive, flexural and tensile strengths of Portland cement-based materials: a systematic literature review. Constr Build Mater. 2020;264:120237.
58. McEuen PL, Fuhrer MS, Park H. Single-walled carbon nanotube electronics. IEEE Trans Nanotechnol. 2002;1(1):78–84.
59. Laurent C, Flahaut E, Peigney A. The weight and density of carbon nanotubes versus the number of walls and diameter. Carbon. 2010;48(10):2994–6.
60. Wen S, Chung DDL. A comparative study of steel- and carbon-fibre cement as piezoresistive strain sensors. Adv Cem Res. 2003;15(3):119–28.
61. Berrocal CG, Hornbostel K, Geiker MR, Löfgren I, Lundgren K, Bekas DG. Electrical resistivity measurements in steel fibre reinforced cementitious materials. Cem Concr Compos. 2018;89:216–29.
62. Bocharov GS, Eletskii AV. Theory of carbon nanotube (CNT)-based electron field emitters. Nanomaterials. 2013;3:393–442.
63. Yoo DY, You I, Lee SJ. Electrical properties of cement-based composites with carbon nanotubes, graphene, and graphite nanofibers. Sensors. 2017;17(5):1064 Available from: https://www.mdpi.com/1424-8220/17/5/1064/htm
64. Nam IW, Souri H, Lee HK. Percolation threshold and piezoresistive response of multi-wall carbon nanotube/cement composites. Smart Struct Syst. 2016;18(2):217–31.
65. Wen S, Chung DDL. Electrical-resistance-based damage self-sensing in carbon fiber reinforced cement. Carbon. 2007;45(4):710–6.
66. Chen PW, Chung DDL. Carbon fiber reinforced concrete for smart structures capable of non-destructive flaw detection. Smart Mater Struct. 1993;2(1):22–30.
67. Azhari F, Banthia N. Cement-based sensors with carbon fibers and carbon nanotubes for piezoresistive sensing. Cem Concr Compos. 2012;34(7):866–73.
68. Tian X, Hu S, Xu Y, Qi H, Xue X. Self-sensing study of stress in low-doped carbon fiber reinforced hydraulic concrete. J Build Eng. 2023;76:107249.
69. Larsen IL, Thorstensen RT. The influence of steel fibres on compressive and tensile strength of ultra high performance concrete: a review. Constr Build Mater. 2020;256:119459.
70. Barabanshchikov Y, Turkebayev A, Dalabayev A, Tleukhanov D. Influence of synthetic fibers dispersed reinforced concrete. Appl Mech Mater. 2015;725–726:543–58. Available from: https://www.scientific.net/AMM.725-726.543
71. Abdullah WA, Mohammed AA, Abdullah AH. Self sensing concrete: a brief review. Int J Adv Mech Civ Eng. 2019;6:2394–827.
72. Hassan A, Elkady H, Shaaban IG. Effect of adding carbon nanotubes on corrosion rates and steel-concrete bond. Sci Rep. 2019;9(1):1–12. Available from: https://www.nature.com/articles/s41598-019-42761-2
73. He W, Hao W, Meng X, Zhang P, Sun X, Shen Y. Influence of graphite powder on the mechanical and acoustic emission characteristics of concrete. Buildings. 2022;12(1):18 Available from: https://www.mdpi.com/2075-5309/12/1/18/htm
74. Kim YA, Hayashi T, Endo M, Dresselhaus MS. Carbon nanofibers. Springer handbook of nanomaterials. Berlin, Heidelberg: Springer; 2013. p. 233–62 Available from: https://link.springer.com/chapter/10.1007/978-3-642-20595-8_7
75. Qiao H, Lin Z, Sun X, Li W, Zhao Y, Guo C. Fiber optic-based durability monitoring in smart concrete: a state-of-art review. Sensors. 2023;23(18):7810.
76. Baptista FG, Budoya DE, de Almeida VAD, Ulson JAC. An experimental study on the effect of temperature on piezoelectric sensors for impedance-based structural health monitoring. Sensors. 2014;14(1):1208–27. Available from: https://www.mdpi.com/1424-8220/14/1/1208/htm
77. Alexander SJ, Sumathi P, Panigrahi SK, Gopalakrishnan N. Embedded dual PZT-based monitoring for curing of concrete. Constr Build Mater. 2021;20(312):125316.
78. Tondolo F, Matta E, Quattrone A, Sabia D. Experimental test on an RC beam equipped with embedded barometric pressure sensors for strains measurement. Smart Mater Struct. 2019;28(5):055040 Available from: https://iopscience.iop.org/article/10.1088/1361-665X/ab1172
79. Tondolo F, Cesetti A, Matta E, Quattrone A, Sabia D. Smart reinforcement steel bars with low-cost MEMS sensors for the structural health monitoring of RC structures. Constr Build Mater. 2018;10(173):740–53.
80. Savino P, Tondolo F. A new approach for displacement and stress monitoring of tunnel based on iFEM methodology. Smart Mater Struct. 2021;31(1):015013 Available from: https://iopscience.iop.org/article/10.1088/1361-665X/ac3901
81. Strangfeld C, Johann S, Bartholmai M. Smart RFID sensors embedded in building structures for early damage detection and long-term monitoring. Sensors. 2019;19(24):5514 Available from: https://www.mdpi.com/1424-8220/19/24/5514/htm
82. Delepine-Lesoille S, Henault JM, Moreau G, Blairon S, Salin J, Courivaud JR, et al. Truly distributed optical fiber sensors for structural health monitoring: from the telecommunication optical fiber drawling tower to water leakage detection in dikes and concrete structure strain monitoring. Adv Civ Eng. 2010;2010:1–13.
83. U.S. Department of Transportation – Federal Highway Administration Research and Technology. Report FHWA-HRT-12-072. Smart Pavement Monitoring System – Chapter 4. Laboratory mechanical testing of the piezoelectric transducer. 2013.
84. Olivera J, González M, Fuente JV, Varga R, Zhukov A, Anaya JJ. An embedded stress sensor for concrete SHM based on amorphous ferromagnetic microwires. Sensors. 2014;14(11):19963–78. Available from: https://www.mdpi.com/1424-8220/14/11/19963/htm
85. Qin L, Lu Y, Li Z. Embedded cement-based piezoelectric sensors for acoustic emission detection in concrete. J Mater Civ Eng. 2010;22(12):1323–7. Available from: https://ascelibrary.org/doi/abs/10.1061/%28ASCE%29MT.1943-5533.0000133
86. Heinrich M, Kroll L, Bauer A. C7.1 – Characterization of carbon fiber-based strain gauge made by embroidery technology for integration in concrete. Proceedings Sensor 2017; 2017 May 30. p. 401–4.

87. Bekzhanova Z, Memon SA, Kim JR. Self-sensing cementitious composites: review and perspective. Nanomaterials. 2021; 11(9):2355.
88. Horszczaruk E, Sikora P, Lukowski P. Application of nanomaterials in production of self-sensing concretes: contemporary developments and prospects. Arch Civ Eng. 2016;62(3):61–74.
89. Liew KM, Kai MF, Zhang LW. Carbon nanotube reinforced cementitious composites: an overview. Compos A: Appl Sci Manuf. 2016;91:301–23.
90. Chang X, Henderson WM, Bouchard DC. Multiwalled carbon nanotube dispersion methods affect their aggregation, deposition, and biomarker response. Environ Sci Technol. 2015; 49(11):6645–53.
91. Vaisman L, Wagner HD, Marom G. The role of surfactants in dispersion of carbon nanotubes. Adv Colloid Interf Sci. 2006; 128–130:37–46.
92. Han B, Yu X, Ou J. Multifunctional and smart carbon nanotube reinforced cement-based materials. In: Gopalakrishnan K, Birgisson B, Taylor P, Attoh-Okine NO, editors. Nanotechnology in civil infrastructure: a paradigm shift [Internet]. Berlin, Heidelberg: Springer; 2011. p. 1–47. https://doi.org/10.1007/978-3-642-16657-0_1
93. Saba AM, Khan AH, Akhtar MN, Khan NA, Rahimian Koloor SS, Petru M, et al. Strength and flexural behavior of steel fiber and silica fume incorporated self-compacting concrete. J Mater Res Technol. 2021;12:1380–90.
94. Nili M, Afroughsabet V. Combined effect of silica fume and steel fibers on the impact resistance and mechanical properties of concrete. Int J Impact Eng. 2010;37:879–86.
95. Zhou ZJ, Yang ZF. Study on the smart property of carbon coated nylon fiber-reinforced concrete composites. Kuei Suan Jen Hsueh Pao/J Chin Ceram Soc. 2001;29(2):192–5.
96. Elseady AAE, Zhuge Y, Ma X, Chow CWK, Lee I, Zeng J, et al. Development of self-sensing cementitious composites by incorporating a two-dimensional carbon-fibre textile network for structural health monitoring. Constr Build Mater. 2024; 415:135049.
97. Wang X, Al-Tabbaa A, Haigh SK. Measurement techniques for self-sensing cementitious composites under flexure. Cem Concr Compos. 2023;142:105215.
98. Han B, Guan X, Ou J. Electrode design, measuring method and data acquisition system of carbon fiber cement paste piezoresistive sensors. Sens Actuators A Phys. 2007;135(2):360–9.
99. Zhang T, Zhang K, Liu W. Exact impact response of multilayered cement-based piezoelectric composite considering electrode effect. J Intell Mater Syst Struct. 2019;30(3):400–15.
100. Li Z, Wei X, Li W. Preliminary interpretation of portland cement hydration process using resistivity measurements. ACI Mater J. 2003;100(3):253–7.
101. Zhang J, Li Z. Application of GEM equation in microstructure characterization of cement-based materials. J Mater Civ Eng. 2009;21(11):648–56.
102. Al-Dahawi A, Yıldırım G, Öztürk O, Şahmaran M. Assessment of self-sensing capability of engineered cementitious composites within the elastic and plastic ranges of cyclic flexural loading. Constr Build Mater. 2017;145:1–10.
103. Gupta S, Gonzalez JG, Loh KJ. Self-sensing concrete enabled by nano-engineered cement-aggregate interfaces. Struct Health Monit. 2017;16(3):309–23.
104. Gonzalez JG, Gupta S, Loh KJ. Multifunctional cement composites enhanced with carbon nanotube thin film interfaces. Proc IEEE. 2016;104(8):1547–60.
105. Smyl D, Hallaji M, Seppänen A, Pour-Ghaz M. Quantitative electrical imaging of three-dimensional moisture flow in cement-based materials. Int J Heat Mass Transf. 2016;103:1348–58.
106. Suryanto B, Saraireh D, Kim J, McCarter WJ, Starrs G, Taha HM. Imaging water ingress into concrete using electrical resistance tomography. Int J Adv Eng Sci Appl Math. 2017; 9(2):109–18.
107. Smyl D. Electrical tomography for characterizing transport properties in cement-based materials: a review. Constr Build Mater. 2020;244:118299.
108. Buasiri T, Kothari A, Habermehl-Cwirzen K, Krzeminski L, Cwirzen A. Monitoring temperature and hydration by mortar sensors made of nanomodified Portland cement. Mater Struct. 2024;57(1):1.
109. Sun MQ, Liew RJY, Zhang MH, Li W. Development of cement-based strain sensor for health monitoring of ultra high strength concrete. Constr Build Mater. 2014;65:630–7. Available from: https://www.infona.pl//resource/bwmeta1.element.elsevier-6c0c5ebe-ba94-34dd-aedf-b6772d4147a4
110. Accornero F, Rubino A, Carpinteri A. Post-cracking regimes in the flexural behaviour of fibre-reinforced concrete beams. Int J Solids Struct. 2022;248:111637.
111. Rubino A, Accornero F, Carpinteri A. Flexural behavior and minimum reinforcement condition in hybrid-reinforced concrete beams. Struct Concr. 2023;24(4):4767–78. Available from: https://onlinelibrary.wiley.com/doi/full/10.1002/suco.202200674
112. Qiu L, Dong S, Yu X, Han B. Self-sensing ultra-high performance concrete for in-situ monitoring. Sens Actuators A Phys. 2021;331:113049.
113. Gawel K, Szewczyk D, Cerasi PR. Self-sensing well cement. Materials. 2021;14(5):1235 Available from: https://www.mdpi.com/1996-1944/14/5/1235/htm
114. Adresi M, Tulliani JM, Lacidogna G, Antonaci P. A novel life prediction model based on monitoring electrical properties of self-sensing cement-based materials. Appl Sci. 2021;11(11): 5080 Available from: https://www.mdpi.com/2076-3417/11/11/5080/htm
115. Çelik DN, Yıldırım G, Al-Dahawi A, Ulugöl H, Han B, Şahmaran M. Self-monitoring of flexural fatigue damage in large-scale steel-reinforced cementitious composite beams. Cem Concr Compos. 2021;123:104183.
116. Xu C, Fu J, Sun L, Masuya H, Zhang L. Fatigue damage self-sensing of bridge deck component with built-in giant piezoresistive cementitious carbon fiber composites. Compos Struct. 2021;276:114459.
117. Ding S, Xiang Y, Ni YQ, Thakur VK, Wang X, Han B, et al. In-situ synthesizing carbon nanotubes on cement to develop self-sensing cementitious composites for smart high-speed rail infrastructures. Nano Today. 2022;43:101438.
118. Ding S, Wang X, Qiu L, Ni YQ, Dong X, Cui Y, et al. Self-sensing cementitious composites with hierarchical carbon fiber-carbon nanotube composite fillers for crack development monitoring of a maglev girder. Small. 2023;19(9):2206258 Available from: https://onlinelibrary.wiley.com/doi/full/10.1002/smll.202206258

119. De Feudis S, Insana A, Barla M, Baccolini L, Zilli L, Mazzola M. Anti-icing using the heat recovered in the Lagoscuro tunnel. In: FABRE 2024. 2024.
120. Sassani A, Ceylan H, Kim S, Gopalakrishnan K, Arabzadeh A, Taylor PC. Influence of mix design variables on engineering properties of carbon fiber-modified electrically conductive concrete. Constr Build Mater. 2017;152:168–81.
121. Sassani A, Arabzadeh A, Ceylan H, Kim S, Gopalakrishnan K, Taylor PC, et al. Polyurethane-carbon microfiber composite coating for electrical heating of concrete pavement surfaces. Heliyon. 2019;5(8):e02359 Available from: http://www.cell.com/article/S2405844019360190/fulltext
122. Lu Y, Zhang J, Li Z, Dong B. Corrosion monitoring of reinforced concrete beam using embedded cement-based piezoelectric sensor. Mag Concr Res. 2015;65(21):1265–76. https://doi.org/10.1680/macr1300071
123. Fouad N, Saifeldeen MA, Huang H, Wu Z. Corrosion monitoring of flexural reinforced concrete members under service loads using distributed long-gauge carbon fiber sensors. Struct Health Monitor. 2017;17(2):379–94. https://doi.org/10.1177/1475921717698973
124. Dong W, Li W, Guo Y, Sun Z, Qu F, Liang R, et al. Application of intrinsic cement-based sensor for traffic detections of human motion and vehicle speed. Constr Build Mater. 2022;355:129130.
125. Abedi M, Fangueiro R, Correia AG. A review of intrinsic self-sensing cementitious composites and prospects for their application in transport infrastructures. Constr Build Mater. 2021;310:125139.
126. Yu Y, Cai CS, Deng L. State-of-the-art review on bridge weigh-in-motion technology. Adv Struct Eng. 2016;19(9):1514–30. Available from: https://journals.sagepub.com/doi/full/10.1177/1369433216655922?casa_token=aPEOqDhvmZQAAAAA%3A-nieFRajUzhKmVMeMk0fNIle5mqfQcY-oDAZWHaeNPU4jVviQvHcheaaKA2mm50KuWQX3sJ7qBtU
127. Ventura R, Barabino B, Vetturi D, Maternini G. Monitoring vehicles with permits and that are illegally overweight on bridges using weigh-in-motion (WIM) devices: a case study from Brescia. Case Stud Transp Policy. 2023;13:101023.
128. Iervolino I, Baltzopoulos G, Vitale A, Grella A, Bonini G, Iannaccone A. Empirical distributions of traffic loads from one year of weigh-in-motion data. Sci Data. 2023;10(1):1–12. Available from: https://www.nature.com/articles/s41597-023-02212-0
129. Gupta S, Lin YA, Lee HJ, Buscheck J, Wu R, Lynch JP, et al. In situ crack mapping of large-scale self-sensing concrete pavements using electrical resistance tomography. Cem Concr Compos. 2021;122:104154 Available from: https://linkinghub.elsevier.com/retrieve/pii/S0958946521002225
130. Gupta S, Gonzalez J, Loh K. Damage detection using smart concrete engineered with nanocomposite cement-aggregate interfaces. 10th International Workshop on Structural Health Monitoring; 2015 September 1–3; Stanford, CA. Destech Publications, Inc; 2015. p. 3033–41.
131. Han B, Zhang K, Burnham T, Kwon E, Yu X. Integration and road tests of a self-sensing CNT concrete pavement system for traffic detection. Smart Mater Struct. 2013;22(1):015020.
132. Coppola L, Buoso A, Corazza F. The influence of AC and DC electrical resistance and piezoresistivity measurements of CNTs/cement composites. 3rd Workshop on the New Boundaries of Structural Concrete; 2013 October 3–4; 2011.
133. Chiarello M, Zinno R. Electrical conductivity of self-monitoring CFRC. Cem Concr Compos. 2005;27(4):463–9.
134. Yoo DY, You I, Zi G, Lee SJ. Effects of carbon nanomaterial type and amount on self-sensing capacity of cement paste. Measurement. 2019;134:750–61.
135. Kim MK, Park J, Kim DJ. Characterizing the electro-mechanical response of self-sensing steel-fiber-reinforced cementitious composites. Constr Build Mater. 2020;240:117954.
136. Hou Y-y, Sun M-q, Chen J-z. Electrical resistance and capacitance responses of smart ultra-high performance concrete with compressive strain by DC and AC measurements. Constr Build Mater. 2022;327:127007.
137. Suchorzewski J, Prieto M, Mueller U. An experimental study of self-sensing concrete enhanced with multi-wall carbon nanotubes in wedge splitting test and DIC. Constr Build Mater. 2020;262:120871.
138. Abedi M, Fangueiro R, Correia AG. Effects of multiscale carbon-based conductive fillers on the performances of a self-sensing cementitious geocomposite. J Build Eng. 2021;43:103171.
139. Lee SH, Kim S, Yoo DY. Hybrid effects of steel fiber and carbon nanotube on self-sensing capability of ultra-high-performance concrete. Constr Build Mater. 2018;185:530–44.
140. Ding Y, Liu G, Hussain A, Pacheco-Torgal F, Zhang Y. Effect of steel fiber and carbon black on the self-sensing ability of concrete cracks under bending. Constr Build Mater. 2019;207:630–9.
141. Wen S, Chung DDL. Effect of admixtures on the dielectric constant of cement paste. Cem Concr Res. 2001;31(4):673–7.
142. Wang Y, Chung DDL. Effect of the fringing electric field on the apparent electric permittivity of cement-based materials. Compos Part B Eng. 2017;126:192–201.
143. Nguyen DL, Song J, Manathamsombat C, Kim DJ. Comparative electromechanical damage-sensing behaviors of six strain-hardening steel fiber-reinforced cementitious composites under direct tension. Compos Part B Eng. 2015;69:159–68.
144. Kim MK, Kim DJ, An YK. Electro-mechanical self-sensing response of ultra-high-performance fiber-reinforced concrete in tension. Compos Part B Eng. 2018;134:254–64.
145. Wang L, Aslani F. Self-sensing performance of cementitious composites with functional fillers at macro, micro and nano scales. Constr Build Mater. 2022;314:125679.
146. Sun S, Han B, Jiang S, Yu X, Wang Y, Li H, et al. Nano graphite platelets-enabled piezoresistive cementitious composites for structural health monitoring. Constr Build Mater. 2017;136:314–28.
147. Cholker AK, Tantray MA. Role of smart concrete in strain sensing and structural properties of reinforced concrete beam. Struct Concr. 2020;21(6):2810–23. Available from: https://onlinelibrary.wiley.com/doi/full/10.1002/suco.202000475
148. Niu Y, Jiao C, Guo W, Li J, Huang H, Huang J, et al. Relation between electrically conductive properties and flexural behaviors of ultra-high-performance concrete. Struct Concr. 2023;24(5):6672–89. Available from: https://onlinelibrary.wiley.com/doi/full/10.1002/suco.202200291

149. You I, Yoo DY, Kim S, Kim MJ, Zi G. Electrical and self-sensing properties of ultra-high-performance fiber-reinforced concrete with carbon nanotubes. Sensors. 2017;17(11):2481.
150. Wang H, Gao X, Liu J, Ren M, Lu A. Multi-functional properties of carbon nanofiber reinforced reactive powder concrete. Constr Build Mater. 2018;187:699–707.
151. Jung M, Park J, Hong S-g, Moon J. Electrically cured ultra-high performance concrete (UHPC) embedded with carbon nanotubes for field casting and crack sensing. Mater Des. 2020;196:109127.
152. Song F, Chen Q, Jiang Z, Zhu X, Li B, He B, et al. Piezoresistive properties of ultra-high-performance fiber-reinforced concrete incorporating few-layer graphene. Constr Build Mater. 2021;305:124362.
153. Al-Najjar Y, Yeşilmen S, Majeed Al-Dahawi A, Şahmaran M, Yildirim G, Lachemi M, et al. Physical and chemical actions of nano-mineral additives on properties of high-volume fly ash engineered cementitious composites. ACI Mater J. 2016; 113(6):791–801.
154. Han D, Hosamo H, Ying C, Nie R. A comprehensive review and analysis of nanosensors for structural health monitoring in bridge maintenance: innovations, challenges, and future perspectives. Appl Sci. 2023;13(20):11149.
155. De Belie N, Gruyaert E, Al-Tabbaa A, Antonaci P, Baera C, Bajare D, et al. A review of self-healing concrete for damage management of structures. Adv Mater Interfaces. 2018;5(17): 1800074.
156. Han B, Yu X, Ou J. Challenges of self-sensing concrete. Self-sensing concrete in smart structures. Oxford: Butterworth-Heinemann; 2014. p. 361–76.
157. Adresi M, Hassani A, Tulliani JM, Lacidogna G, Antonaci P. A study of the main factors affecting the performance of self-sensing concrete. Adv Cem Res. 2017;29(5):216–26.
158. Yıldırım G, Öztürk O, Al-Dahawi A, Afşın Ulu A, Şahmaran M. Self-sensing capability of engineered cementitious composites: effects of aging and loading conditions. Constr Build Mater. 2020;231:117132.
159. Adresi M, Pakhirehzan F. Evaluating the performance of self-sensing concrete sensors under temperature and moisture variations – a review. Constr Build Mater. 2023;404:132923.
160. Wen S, Chung DDL. Self-sensing of flexural damage and strain in carbon fiber reinforced cement and effect of embedded steel reinforcing bars. Carbon. 2006;44(8):1496–502.
161. Nalon GH, Lopes Ribeiro JC, Duarte de Araújo EN, Marcio da Silva R, Pedroti LG. Effects of shrinkage-reducing admixtures and expansive agents on the self-sensing behavior of nanomodified cement-based materials. J Build Eng. 2023;78:107648.
162. Konsta-Gdoutos MS, Aza CA. Self sensing carbon nanotube (CNT) and nanofiber (CNF) cementitious composites for real time damage assessment in smart structures. Cem Concr Compos. 2014;53:162–9.
163. Liu H, Laflamme S, D'Alessandro A, Ubertini F. 3D printed self-sensing cementitious composites using graphite and carbon microfibers. Meas Sci Technol. 2024;35:085105 Available from: https://iopscience.iop.org/article/10.1088/1361-6501/ad41f9
164. Gamil Y. Machine learning in concrete technology: a review of current researches, trends, and applications. Front Built Environ. 2023;9:1145591.
165. Ubertini F, D'Alessandro A. Concrete with self-sensing properties. Eco-efficient repair and rehabilitation of concrete infrastructures. Cambridge: Woodhead Publishing; 2018. p. 501–30.
166. Liu Z. Book review of self-sensing concrete in smart structures. Eng Mater Struct. 2023;2(1):15–7.
167. Soltani E, Ahmadi E, Gueniat F, Salami MR. A review of bridge health monitoring based on machine learning. Proceedings of the Institution of Civil Engineers: Bridge Engineering. 2022.
168. Kurian B, Liyanapathirana R. Machine Learning Techniques for Structural Health Monitoring. In: Wahab, M. (eds) Proceedings of the 13th International Conference on Damage Assessment of Structures. Lecture Notes in Mechanical Engineering. Singapore: Springer; 2020.
169. Kekez S. Use of artificial neural networks for prediction of properties of self-sensing concrete. Proceedings of the 6th World Congress on Civil, Structural, and Environmental Engineering (CSEE'21), Virtual Conference – June 21 – 23, 2021. Paper No. ICSECT 106; 2021. doi:10.11159/icsect21.lx.106
170. Quqa S, Landi L, Loh KJ. Crack identification using electrical impedance tomography and transfer learning. Comput Aided Civ Inf Eng. 2023;38(17):2426–42.
171. Papanikolaou I, Al-Tabbaa A, Goisis M. An industry survey on the use of graphene-reinforced concrete for self-sensing applications. International Conference on Smart Infrastructure and Construction 2019, ICSIC 2019: Driving Data-Informed Decision-Making; 2019. p. 613–22. Available from: https://www.icevirtuallibrary.com/doi/10.1680/icsic.64669.613
172. Papanikolaou I, Davies A, Jin F, Litina C, Al-Tab-Baa A. Graphene oxide/cement composites for sprayed concrete tunnel linings – ITA Library. 2017 Available from: https://library.ita-aites.org/wtc/1454-graphene-oxide-cement-composites-for-sprayed-concrete-tunnel-linings.html

AUTHOR BIOGRAPHIES

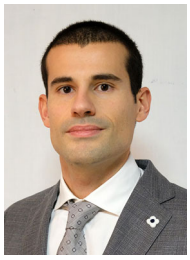

Marco Civera, Department of Structural, Building and Geotechnical Engineering, Politecnico di Torino, Corso Duca degli Abruzzi 24, 10129 Turin, Italy. Email: marco.civera@polito.it

Ahmad Naseem, Department of Structural, Building and Geotechnical Engineering, Politecnico di Torino, Corso Duca degli Abruzzi 24, 10129 Turin, Italy. Email: anaseem4588@gmail.com

Bernardino Chiaia, Department of Structural, Building and Geotechnical Engineering, Politecnico di Torino, Corso Duca degli Abruzzi 24, 10129 Turin, Italy. Email: bernardino.chiaia@polito.it

How to cite this article: Civera M, Naseem A, Chiaia B. Recent advances in embedded technologies and self-sensing concrete for structural health monitoring. Structural Concrete. 2025;26(5):5300–34. https://doi.org/10.1002/suco.202400714